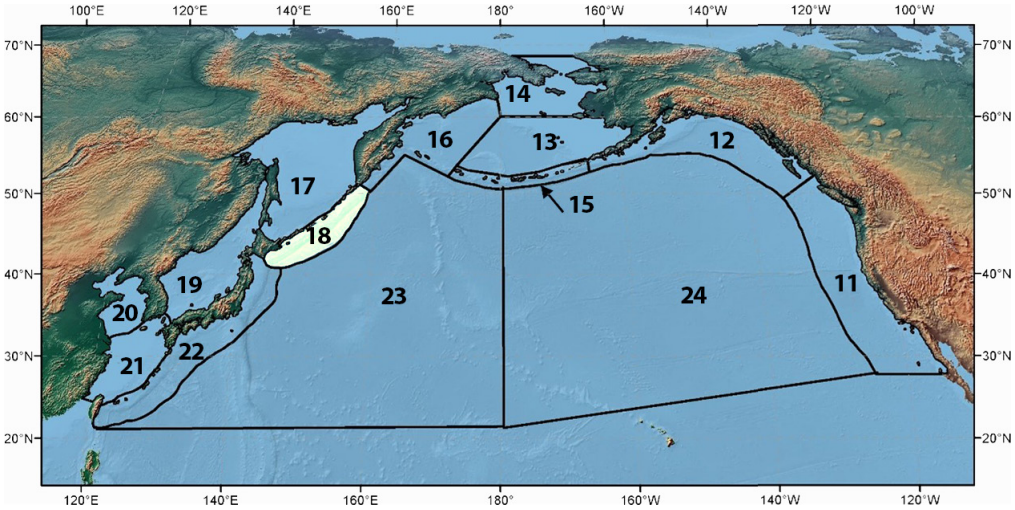

PICES

Regional Report for PICES Region:

18

PICES SPECIAL PUBLICATION 7

Marine Ecosystems of the North Pacific Ocean 2009–2016

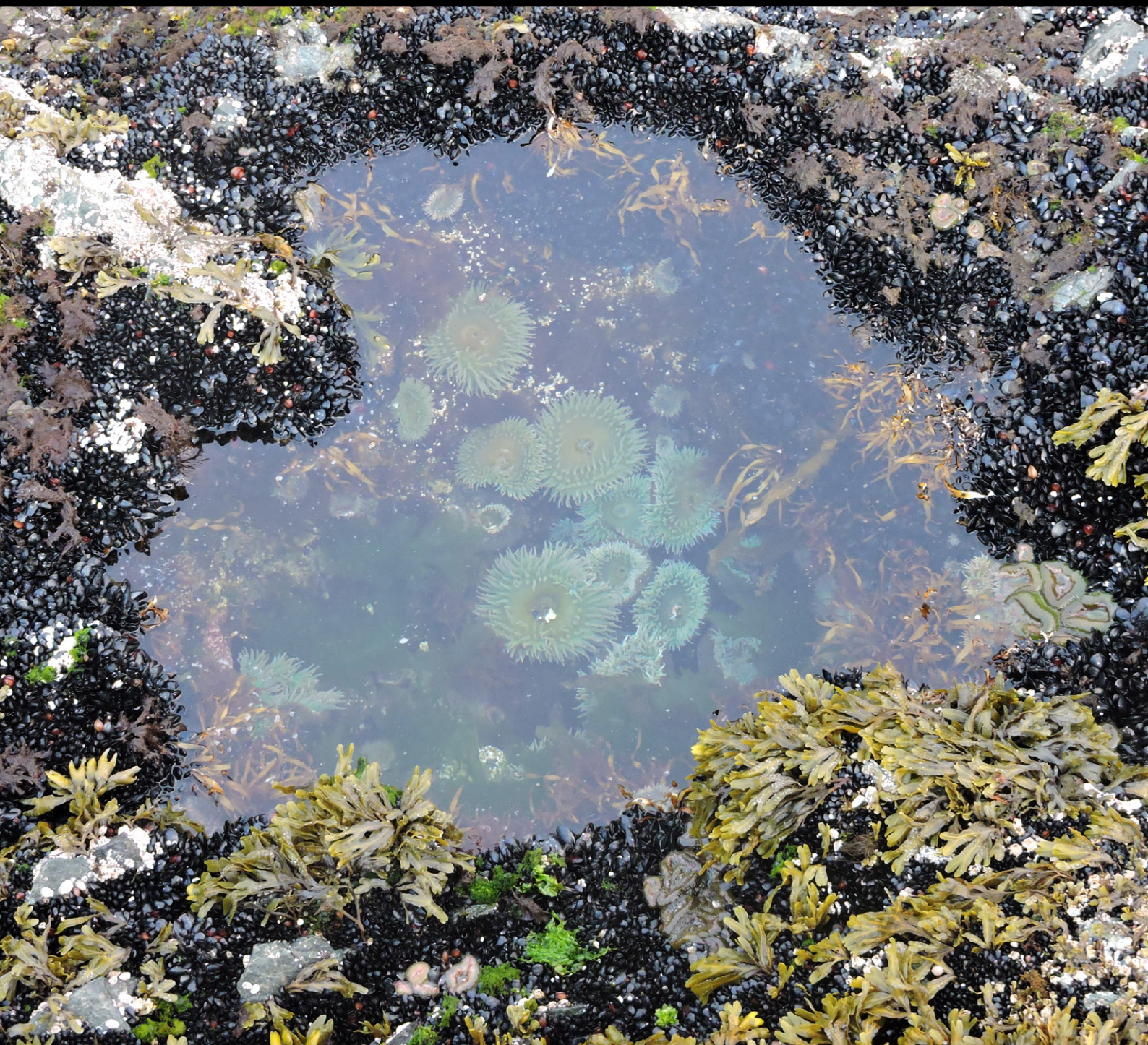

PICES North Pacific Ecosystem Status Report, Region 18 (Oyashio)

Hiroshi Kuroda
Fisheries Resources Institute (Kushiro),
Japan Fisheries Research and Education Agency (FRA),
Hokkaido, Japan

Contributors: Kuroda, H[1]., Mitsudera, H[2]., Sugimoto, S[3]., Suga, T.[3], Kakehi, S.[1], Kasai, H.[1], Sasano, D.[4], Ono, T.[1], Kaeriyama, H.[1], Taniuchi, Y.[1], Tadokoro, K.[1], Okazaki, Y.[1], Furuichi, S.[1,] Yukami, R.[1,] Kamimura,Y.[1], Kaga, T.[1], Kidokoro, H.[1], Saito, T.[1], Watanuki, Y.[5], Yamamura, O.[5]

[1]Fisheries Resources Institute, Japan Fisheries Research and Education Agency
[2]Institute of Low Temperature Science, Hokkaido University
[3]Graduate School of Science, Tohoku University
[4]Atmosphere and Ocean Department, Japan Meteorological Agency
[5]Graduate School of Fisheries Sciences, Hokkaido University

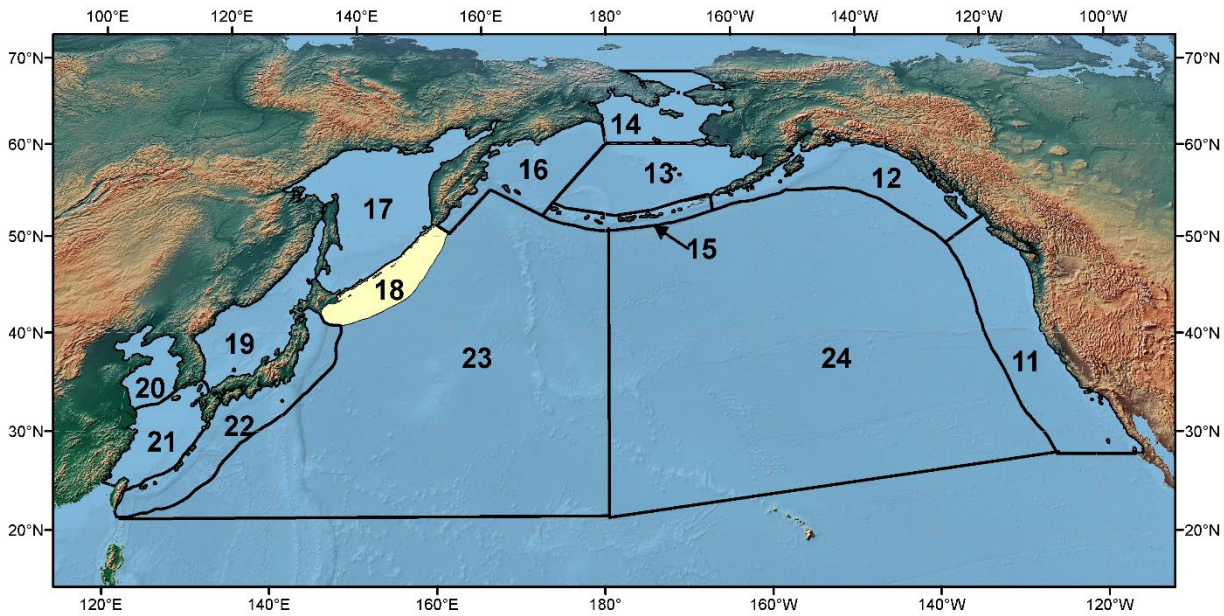

Figure R18-1. The PICES biogeographical regions and naming convention for the North Pacific Ocean with the area discussed in this report highlighted.

1. Highlights

- The PDO index shows an abrupt phase reversal to positive around 2013/14, which implies that a regime shift similar to 1956/1957 and 1976/1977 occurred.
- After 2013, the center of the Aleutian Low shifted eastward by 25° in longitude, which likely induces northerly (southerly) wind with cold (warm) air in the central (eastern) North Pacific, leading to SST cooling (warming).
- The Oyashio transport on the slope off the Hokkaido coast decreased interdecadally after 1993, because of stagnation of mesoscale clockwise eddies off the Hokkaido coast and northward shift of the gyre boundary.
- The southernmost latitude of the First Oyashio Intrusion abnormally shifted northward to 41–43°N during 2015–2016 and seemed to return to the south after March 2017.
- Nutrient concentrations at the sea surface in the main stream of the Oyashio exhibited an interdecadal increase in January (pre-bloom period) and decrease in July (post-bloom period) after 1990.
- Chlorophyll *a* concentrations at the sea surface in January also showed an interdecadal increase.
- Significant trends toward decreasing O_2 have been found on isopycnal surfaces between 26.6 and 27.4 σ_θ.
- The hypoxia boundary shoaled from 680 m in 1951 to 560 m in 2010, which seemed to correspond to the fact that the deepest catch of Pacific cod changed from 720 m in 1957 to 575 m in recent 10 years.
- After the Fukushima accident, the concentration of ^{137}Cs had been increased up to 70±4.2 Bq m^{-3} in September 2011, rapidly decreased until May 2012, and then mostly returned to the background level before the accident.
- Concentrations of size-fractionated chlorophyll *a* clarified that the small fraction < 2 μm was dominant in all seasons except the spring, although the large fraction > 10 μm was frequently highlighted due to major composition of phytoplankton in spring bloom.
- Mesozooplankton communities associated with the Kuroshio-Oyashio Transition and Kuroshio waters expanded extensively northward in summer–autumn of 2015 and 2016, when the First Oyashio Intrusion weakened abnormally.
- Euphausiids biomass was negatively correlated with temperature at the depth of 200 m and declined in 2008, 2010, and after 2013, associated with a high temperature in the subsurface.
- Good recruitment of sardine has occurred since 2010, and the spawning stock biomass and catch have been increasing in recent years.
- Catch and biomass of sardine seem to be negatively related with those of anchovy and flying squid.
- The catch of Pacific saury by Japanese fisheries tended to decrease after 2010.
- Chum salmon catches have decreased further since 2010 on the Hokkaido and Honshu Pacific sides, the reasons of which have not been identified.
- Pink salmon catch decreased during 2011–2015 probably due to low SSTs during coastal residency of juveniles and high SSTs during spawning migrations of adults and/or loss of diversity of spawning timing caused by artificial selection for early spawning fish in hatcheries.
- Four species of alcids showed contrasting population trends in the 2010s along the Pacific coast of eastern Hokkaido; Common Murres and Tufted Puffins that showed a large decline in the 1970s did not recover, whereas Spectacled Guillemots and Rhinoceros Auklets seemed to increase slightly in the 2010s.
- In 2016, pup production of Steller sea lions decreased in Kuril Islands after 20 years of increasing trend, while those in Sakhalin and northern Okhotsk continued to increase.

2. Introduction

(Mitsudera)

The Oyashio is a western boundary current of the subarctic gyre in the North Pacific, whose upstream region is usually called the East Kamchatka Current originating in the Bering Sea. The Oyashio water is transformed greatly as it flows along the Kuril Islands by vigorous tidal mixing and the outflow from the Sea of Okhotsk (Yasuda 1997). A part of the Oyashio intrudes southward into the subtropical gyre and finally becomes a source water of the North Pacific Intermediate Water (NPIW) (Yasuda et al. 1996). Another part of the Oyashio turns northeastward and becomes the Oyashio Return Flow (or often referred to as the Subarctic Current).

It is well known that the Oyashio off the east coast of Hokkaido exhibits complicated hydrographic structures because of the confluence between the warm and saline Kuroshio water and the cold and fresh Oyashio water. Nevertheless, recent analyses of satellite observations, hydrographic observations and velocity measurements reveal that the flow field is well characterized by a series of organized mean flows, including a southwestward flow relating to the First Oyashio Intrusion, a northeastward flow over the Kuril-Kamchatka Trench, another southwestward flow associated with the Second Intrusion, and a stable northeastward flow corresponding to the Oyashio Return Flow (Kuroda et al. 2017). The Oyashio transport off Hokkaido decreased remarkably during the past decades (1993–2011), caused by the frequent appearance of clockwise warm eddies originating in the Kuroshio, and the decrease was probably linked with the recent northward shift of the gyre boundary associated with the interdecadal weakening of the Aleutian Low (Kuroda et al. 2015).

Stable, organized flows were also found in the Transitional Domain (TD) farther to the east, which is a boundary between the subtropical gyre and subarctic gyre of the North Pacific, although the region is known as a region of complex mixed waters. Isoguchi et al. (2006) found two stationary jets that transport the Kuroshio water into the TD. Particularly, the western jet, called J1, flows northeastward in contact with the Oyashio Return Flow, forming a sharp temperature-and-salinity in-between (Wagawa et al. 2014; Kida et al. 2015). This is the Subarctic Front, or the Oyashio Front, identified usually by the 4 ºC contour at a depth of 100 m as a proxy.

The organized flow field in the Oyashio off Hokkaido and the stationary jets in the TD must be important for material transport associated with biogeochemical cycles, as well as heat and salt transport across the subtropical-subarctic gyre boundary. These currents appear to exist over sea-floor elevations whose amplitude is as high as ~500 m, except for the northeastward flow over the Kuril-Kamchatka Trench. It is curious why such small-amplitude topographic features can anchor the surface currents in the deep Pacific Ocean (~6000 m). A theoretical modeling effort is in progress from a point of view of geostrophic turbulence over topography and baroclinic Rossby wave characteristics (Miyama et al. 2018; Mitsudera et al. 2018).

3. Atmosphere

(Sugimoto, Suga)

3.1. Regime shift

The climate system in the North Pacific exhibits long-term variations on decadal and interdecadal time scales (Mantua et al. 1997; Minobe 1999). Because the phase reversals of such long-term variations appear like a step function rather than a sinusoidal function, these reversals are often called a 'climate jump' or 'regime shift'. Specifically, a regime shift is an abrupt transition from one quasi-steady climatic state to another, with the transition period being much shorter than the duration of each state. Such regime shifts occur not only in sea surface temperature (SST) and atmospheric fields, such as sea level pressure (SLP), but also in the marine ecosystem and fisheries (Mantua et al. 1997). At least six regime shifts occurred in the 20th century, during 1925/26, 1942/43, 1957/58, 1970/71, 1976/77, and 1997/98 (Minobe 1997, 1999, 2002; Zhang et al. 1997; Yasunaka and Hanawa 2002, 2003, 2005; Yeh et al. 2011; Jo et al. 2013).

3.2. Evidence for a regime shift in 2013/14

To determine whether or not a regime shift has occurred since the 1997/98 event, we investigated the Pacific Decadal Oscillation (PDO), which is the dominant mode of climate variability in the North Pacific SST field (Zhang et al. 1997) and has important impacts on the marine ecosystem and fisheries (Mantua et al. 1997). The PDO index (Figure R18-2a) shows an abrupt phase reversal around 2013/14. The difference in the index value between January 2009–December 2013 and January 2014–July 2017 is 2.08, larger than that of any previous regime shifts (the difference between consecutive 5-year periods is 1.03 for 1953–1957and 1958–1962, −0.47 for 1966–1970 and 1971–1975, 1.10 for 1972–1976 and 1977–1981, and −1.15 for 1993–1997 and 1998–2002). This abrupt reversal implies that a regime shift occurred around 2013/14. To further investigate whether or not a regime shift occurred at this time, we identified years when significant shifts occurred in the North Pacific SST field, without any prescribed spatial patterns related to known regime shifts. Here, we used the winter SST of January–March because this is known season of regime-shift occurrence (e.g., Yasunaka and Hanawa 2005), and we used the difference between 5-year means before and after a given year as an indicator of the shift. The averaging time of 5 years was selected to reduce influences from relatively high-frequency variations such as El Niño, which has a typical time scale of 3–4 years. Then, the number of grid points in which the difference between means before and after a given year changes by more than 10% significance level was counted. Figure R18-2b presents a time series of the ratio of these grid points to the total number of grid points over the North Pacific. This detection method successfully identifies major shifts that occurred in the second half of the 20th century. Furthermore, it is found that the ratio in 2013/14 is the highest in the 21st century and ranks second since 1950 overall. Thus, there is an extremely high possibility that a regime shift occurred in 2013/14 in the North Pacific.

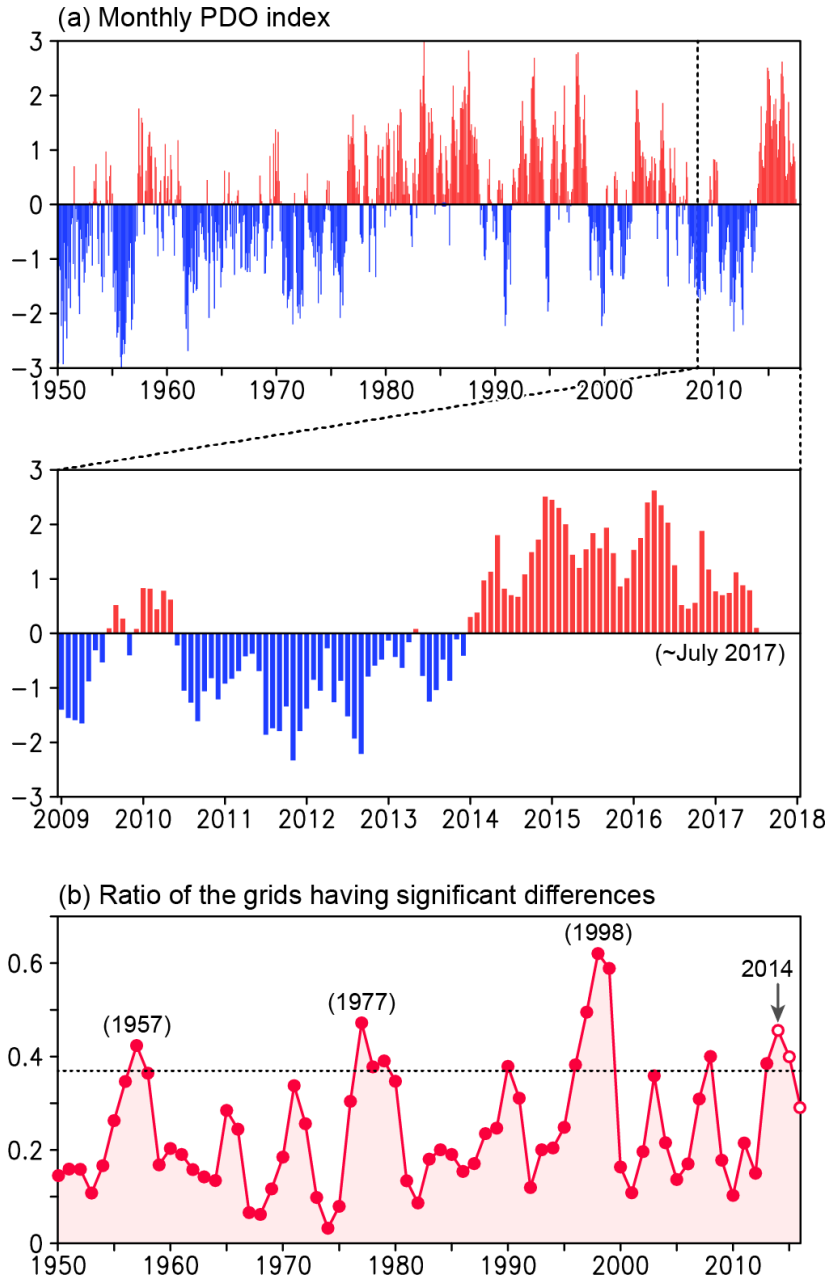

[Figure R18-2] (a) Time series of the PDO index, from the NOAA web site. (b) Time series of the ratio of grid points that undergo a significant difference in 5-year means before and after a particular year in the winter (January–March) SST field in the North Pacific (0°–60°N, 120°–260°E), from NOAA's extended reconstruction of SSTs (ERSSTv4; Huang et al. 2014). For example, the value for the year 2000 is the difference between 1995–1999 and 2000–2004. White circles indicate years since 2014 when the number of years used in the calculation is < 5. Horizontal dashed line indicates the mean plus one standard deviation of ratio.

The winter SST difference associated with this latest regime shift (Figure R18-3a) represents strong negative values in the central North Pacific and positive values along the west coast of North America that extend to the equatorial Pacific. The SLP difference represents large negative anomalies in the central/eastern North Pacific, which result from an eastward shift of the Aleutian Low (AL) center by 25° in longitude (Figure R18-4). The AL center was located at 170°E in winter during 2009–2013, but at 165°W in winter during 2014–2017. The AL eastward shift likely induces northerly (southerly) wind with cold (warm) air in the central (eastern) North Pacific, leading to SST cooling (warming). Both the SST and SLP patterns during 2013/14 are similar to those during regime shifts in 1956/57 and 1976/77 (Figure R18-3).

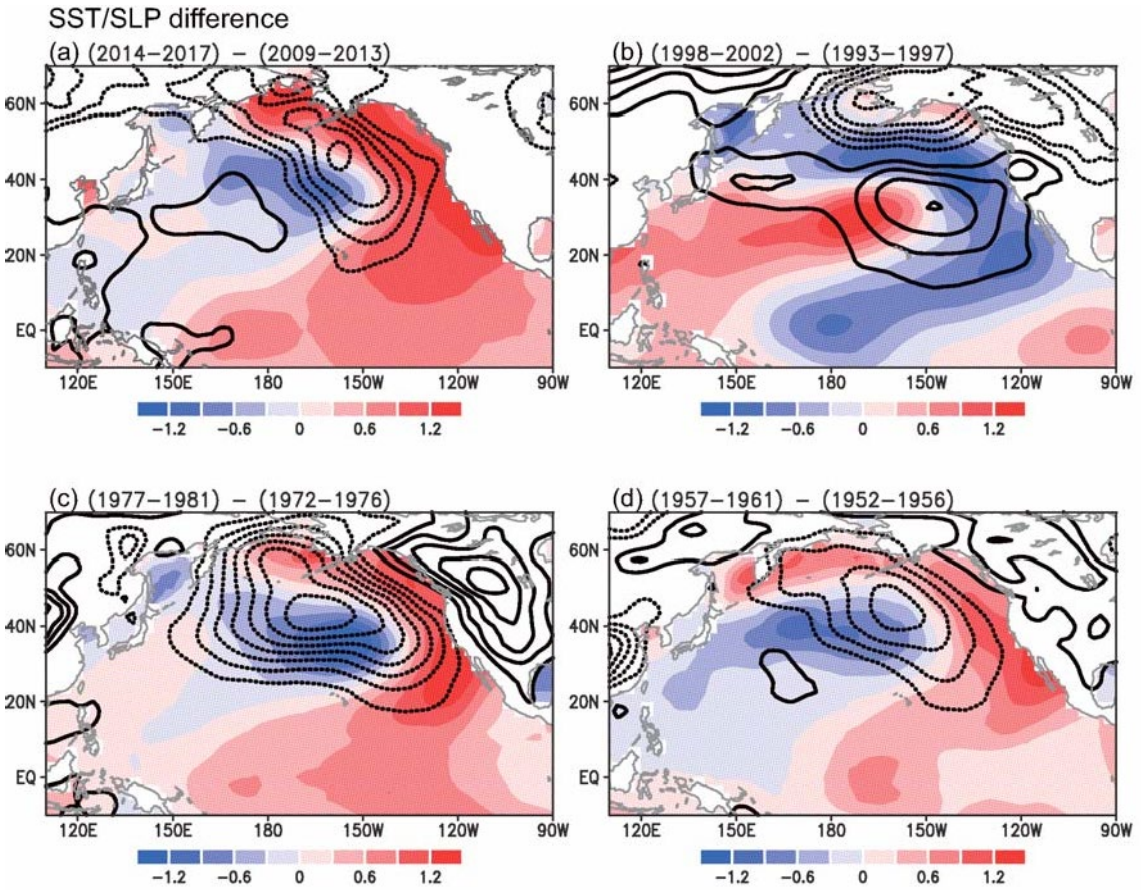

[Figure R18-3] Difference map of winter SST (January–March) between consecutive 5-year periods for each regime shift (colors), from ERSSTv4: (a) 2013/14, (b) 1997/98, (c) 1976/77, and (d) 1956/57. Black contours indicate the winter SLP difference (December–February) from the NCEP/NCAR reanalysis dataset (Kalnay et al. 1996). The contour interval is 1 hPa and zero contours are omitted.

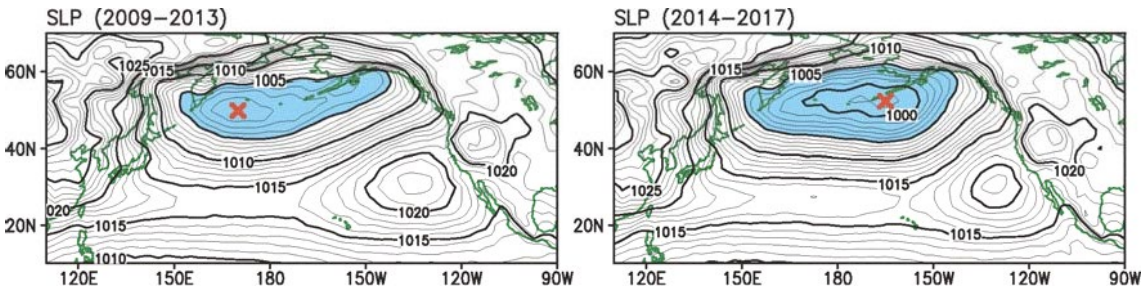

[Figure R18-4] Winter SLP during (left panel) 2009–2013 and (right panel) 2014–2017. The contour interval is 1 hPa. Shading denotes regions with SLP < 1005 hPa. The AL center, defined as the location of minimum SLP, is indicated by (×)

Previous studies have reported that regime shifts in the 20th century have been concurrent with El Niño events, which suggests that El Niño events may act as a trigger for regime shifts (e.g., Yasunaka and Hanawa 2005). The latest El Niño event, which occurred in summer 2014, and took the mature phase in December 2015, had the second largest magnitude on record (Figure R18-5). The concurrence of these latest regime shift and El Niño events lends further support to the possibility that El Niño events are important factors in the occurrence of regime shifts.

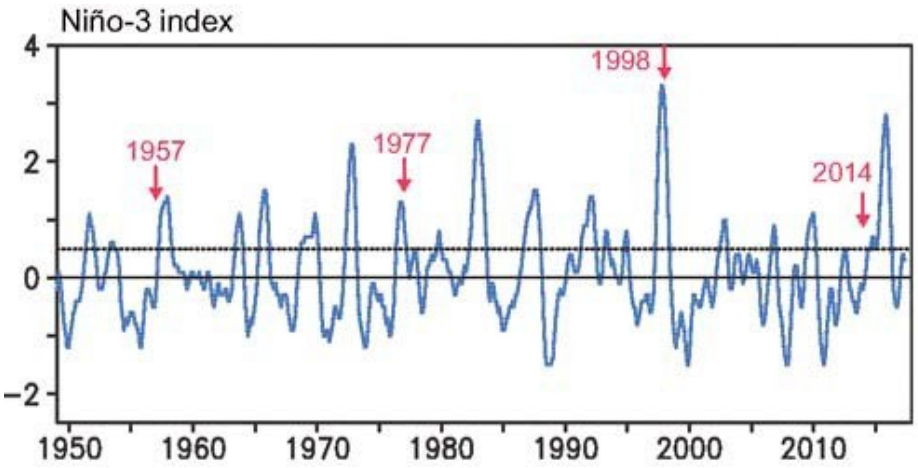

[Figure R18-5] Time series of the Niño-3 index, from the Japan Meteorological Agency (JMA) website. The years indicated with arrows are those associated with the North Pacific regime shifts shown in Figure R18-2b.

In the western North Pacific, including the Oyashio, the SST response during 2013/14 was smaller than that during other regime-shift periods (Figure R18-3). However, it is expected that the influence of an AL change in 2013/14 would be noticed in the western North Pacific in the late 2010s because of delayed ocean-adjustment processes related to baroclinic Rossby wave propagation that occurs as a result of the AL change. Thus, it will be important to monitor the western North Pacific in the coming few years to identify this change and mitigate regime shift damage to the marine ecosystem and fisheries as soon as possible.

4. Physical Oceanography

(Kakehi)

The Fisheries Resources Institute (Shiogama) defines the Oyashio region as the area that is < 5 ºC at 100-m depth. The southernmost position of the Oyashio coastal intrusion (the First Oyashio Intrusion; OY1) varies every year (Figure R18-6a). From 2009 to 2014, the position fluctuated around the climatological latitude (calculated as 40.0°N from 1960 to 2016), although sporadic northward or southward shifts occurred (Figure R18-6c). From June 2015 to June 2016, the position persistently shifted northward and was located at 41–43°N. The 13-month running mean latitude of OY1 was the highest in February 2016 (41.8°N) since 1960. The second closest to the coastal intrusion of the Oyashio (the Second Oyashio Intrusion; OY2) was also located on the climatological latitude (39.5 °N) from 2009 to 2014 and shifted northward in 2015 (Figure R18-6d). Because of these northward shifts of the Oyashio, the migration of chum salmon (*Oncorhynchus keta*) and Pacific saury (*Cololabis saira*) to the nearshore region of Japan was blocked in 2015 and 2016. The northward shifts were caused by an anti-cyclonic eddy (warm core ring [WR]) that was located off the southeastern Hokkaido Island (the so-called Doto area) (Figure R18-7). The WR named WR-2010G by the Fisheries Resources Institute (Shiogama) occurred on August 2010 on the northern side of the Kuroshio Extension (37°N, 145°E), moved northward from 2010 to 2011, and stayed off Hokkaido Island during 2012–2016 (Figure R18-8). From 2015 to 2016, when the OY1 shifted extremely northward, the WR-2010G extended to the nearshore of Hokkaido Island, although its center position was approximately the same as that of previous years (Figure R18-7). The WR-2010G started to move northeastward on October 2016 and vanished on February 2017. Such a long-lived WR is unprecedented; therefore, the mechanisms of maintaining the structure of the WR so that it survives the winter several times over is an issue to be addressed in future. The southernmost latitude of the OY1 moved south from March 2017 and reached the average latitude on April 2017 for the first time in 2 years.

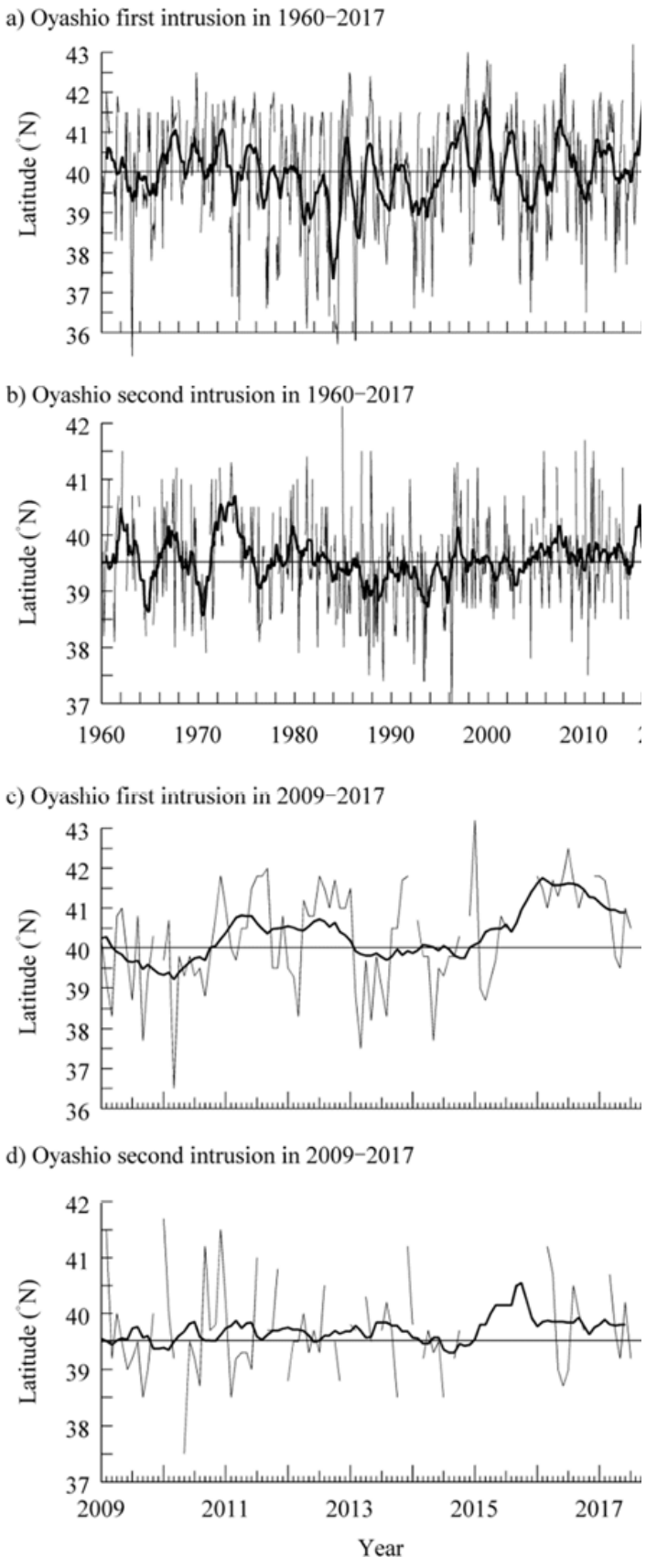

[Figure R18-6] Time series of the southernmost latitude of the First (a) and Second (b) Oyashio Intrusion defined as the region that is < 5 ºC at 100-m depth (https://ocean.fra.go.jp/temp/temp.html) in 1960–2017. Thin and thick lines indicate monthly values and the 13- month running mean, respectively. (c) and (d) indicate those in 2009–2017.

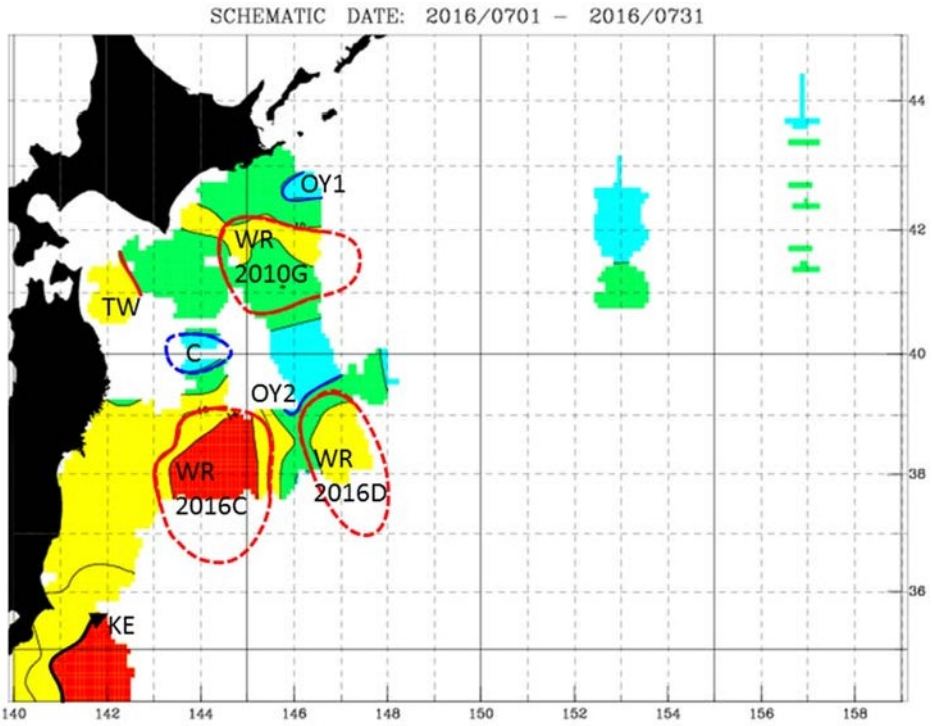

[Figure R18-7] Shown here are First Oyashio Intrusion (OY1), the Second Oyashio Intrusion (OY2), the anti-cyclonic eddy (warm core ring -WR), the Kuroshio Extension (KE), the cyclonic eddy (cold core ring- C, and the Tsugaru warm water (TW), The solid colours red, yellow, green, and blue regions indicate the KE area (red-$T \geq 14$ °C at 200-m depth), warm water derived from the KE (yellow -$T < 14$ °C at 200-m depth, and $T \geq 10$ °C at 100-m depth), mixed water between the KE and the Oyashio (green - $5 \leq T < 10$ °C at 100-m depth), and the Oyashio (blue -$T < 5$ °C at 100-m depth).

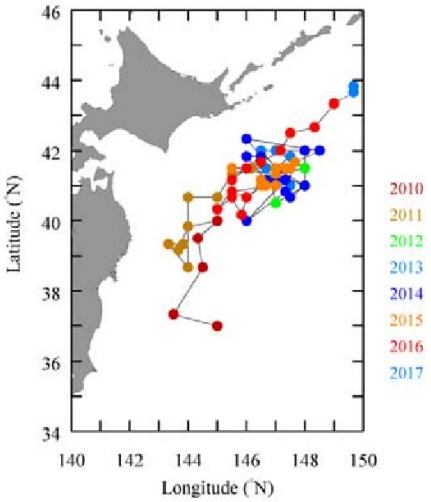

[Figure R18-8] The trajectory of the center position of the warm core ring (WR-2010G), which was first identified in August 2010. Colors indicate years.

5. Chemical Oceanography

5.1. Nutrients

(Kasai)

The Japan Fisheries Research and Education Agency (FRA) has regularly conducted oceanographic surveys to monitor the Oyashio conditions since 1987 along a transect of about 500-km length that extends southeastward from the southeastern coast of Hokkaido (Akkeshi Bay), which is referred to as “A-line” (Figure R18-9). Stn. A01 is the closest to the Hokkaido coast and on the continental shelf, and Stn. A21 is the most offshore and in the Kuroshio-Oyashio Transition zone. The A-line monitoring was carried out on average five times a year, with ADCP (Acoustic Doppler Current Profiler), CTD (Conductivity Temperature Depth), some nets for sampling zooplankton, and water sampler to measure biochemical parameters such as chlorophyll *a*, nutrient, and dissolved oxygen concentrations. Routinely-monitored data on the A-line are distributed from a website (https://ocean.fra.go.jp/a-line/a-line_index2.html)) and some parts of the A-line data were used in this report to describe the recent status of the Oyashio region.

Generally, the most remarkable feature in dynamics of nutrients in the Oyashio region is characterized by large seasonal variability in the surface mixed layer. Annual maximum of nutrient concentrations appears in winter. The nutrient concentrations decrease rapidly during spring due to large-scale phytoplankton bloom (Saito et al. 2002). Nutrient concentrations are depleted to low level during summer to autumn. After late autumn, seasonal stratification in the surface layer is broken by intensified vertical convection associated with strong wind and cooling at the sea surface. As a result, nutrients are entrained into the mixed layer from the subsurface layer beneath the bottom of mixed layer.

At the sea surface, the maximum concentration of nitrate in the main stream of the Oyashio on the continental slope (Stn. A03–A07 on the A-line) was observed in January and March (Figure R18-10). The nitrate concentrations during winter were higher in the main stream area than those in adjacent waters. During summer and autumn, nitrate concentrations reached their annual minimum (2–3 μM for nitrate). The decline of nitrate concentration from March to May, which corresponds to the period of the spring bloom of phytoplankton, was about 10 μM for nitrate. This decline was comparable between in the shelf to shelf-edge area (Stn. A01–A02) and in the main stream area on the slope (Stns. A03–A07). On the other hand, the decrease of nitrate concentration after May was higher in the main stream area than in the shelf to shelf-edge area. This implies differences in dynamics of spring bloom between the two areas.

Monthly mean concentrations of nitrate were estimated by changing average periods: such as during 1990–2014, 1990–1996, 1997–2002, 2003–2008, and 2009–2014. A remarkable difference in decline of nitrate concentrations during the spring bloom (March–May) are not apparent between for the recent years of 2009–2014 and the other periods. However, the nitrate concentrations in May seemed to be different among the mean periods, which suggests the presence of interannual variability in occurrence time and magnitude of phytoplankton bloom.

Using the long term dataset from oceanographic monitoring surveys, some previous studies reported linear trends in variability of nutrient concentration within surface mixed layer in the subarctic region of the North Pacific. Ono et al. (2002) reported a decrease of phosphate concentrations in the mixed layer, using a dataset from the 1960s to the 1990s. Moreover, Whitney (2011) showed there were significant trends, namely, the increase of nitrate and phosphate concentrations in the Bering Sea. Their analysis also indicated that there was no significant trend in the western subarctic region including the Oyashio region.

However, we detected significant interdecadal increases of nutrient concentrations at the sea surface in January (i.e., pre-bloom period) after 1990 on the A-line for both the shelf to shelf

edge and the main stream of the Oyashio region on the slope (Figure R18-11). In contrast, interdecadal decreases of nutrient concentrations at the sea surface were detected in July (post-bloom period). The decreases were statistically significant only for the main stream of the Oyashio region. The slopes of the regression line in January were estimated as 0.15–0.16 μM yr^{-1} for nitrate, 0.019–0.021 μM yr^{-1} for phosphate, and 0.39–0.47 μM yr^{-1} for silicate. These trends imply that there were interdecadal variations in nutrient supply to the surface layer and/or consumption of nutrients by primary production. The possible process and mechanism of the interdecadal variability are unclear and need to be clarified in future work. It is moreover noteworthy that the significant interdecadal variations of nutrient concentrations were limited to the sea surface and hardly appeared in the subsurface layer of 26.8–26.9 σ_t (Figure R18-12).

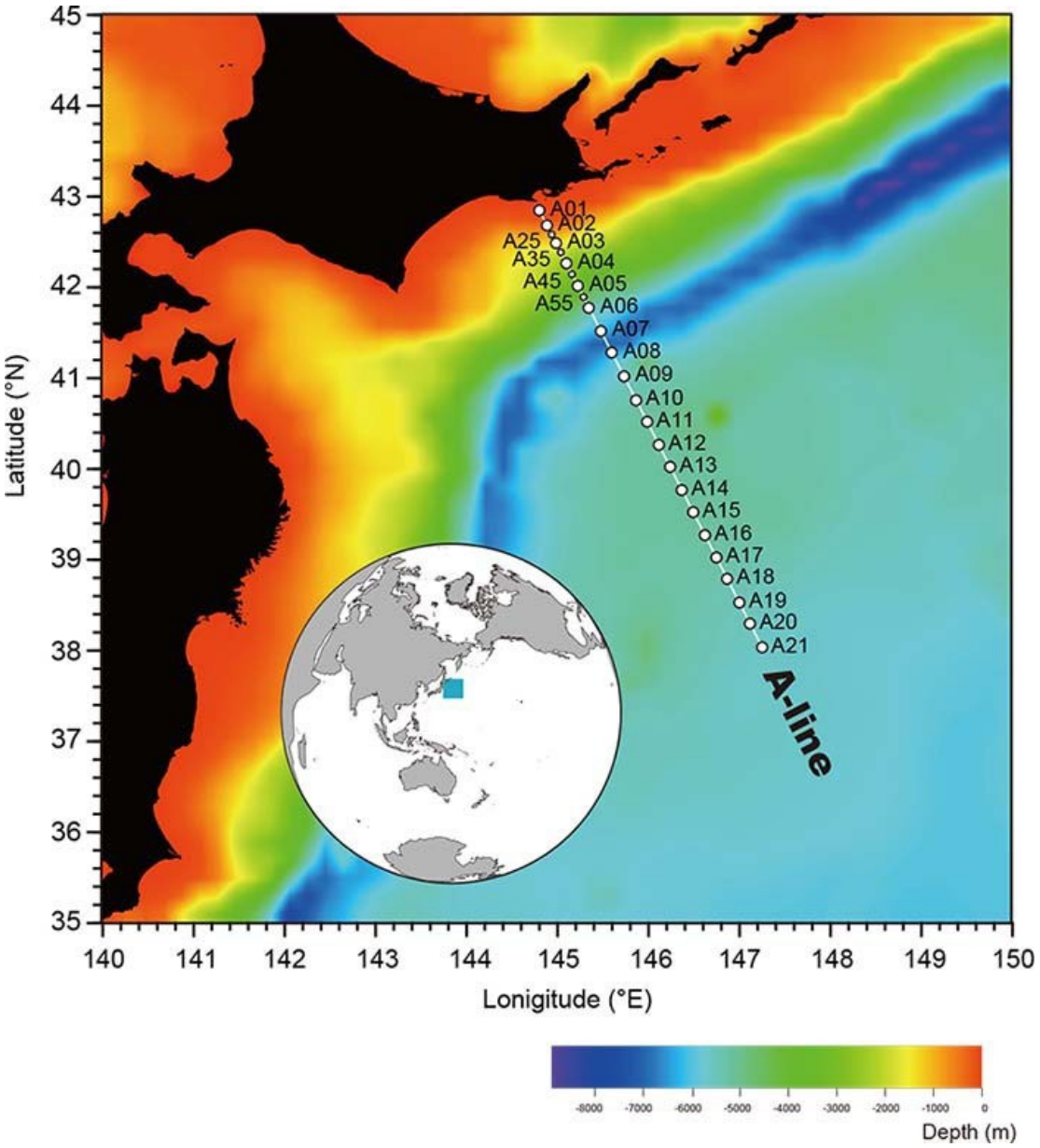

[Figure R18-9] Regular monitoring transect of the A-line off the southeastern coast of Hokkaido.

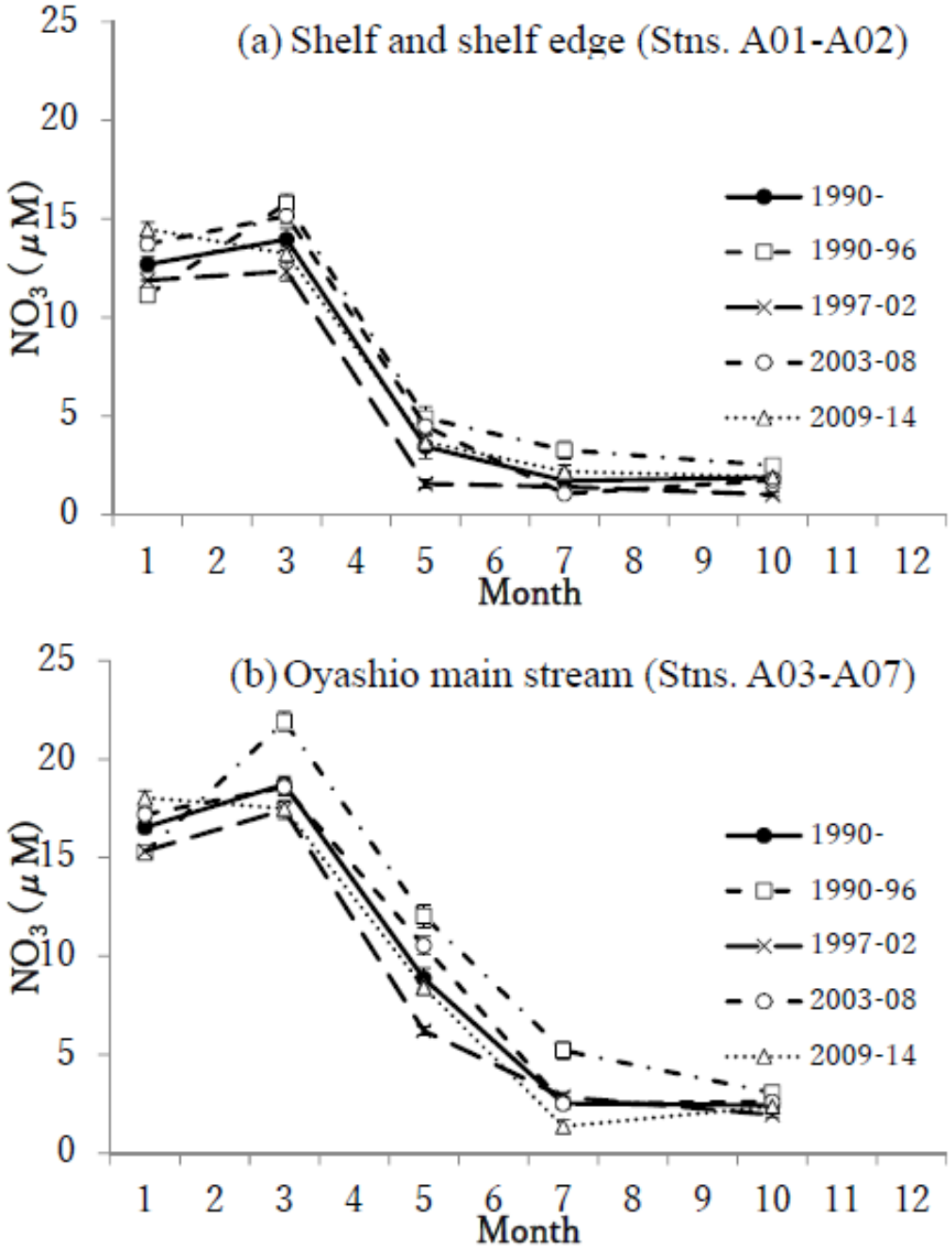

[Figure R18-10] Monthly means of nitrate concentrations at the sea surface averaged for five different periods (a) on the shelf to shelf edge (Stns. A01–A02) and (b) in the main stream of the Oyashio on the slope (Stns. A03–A07).

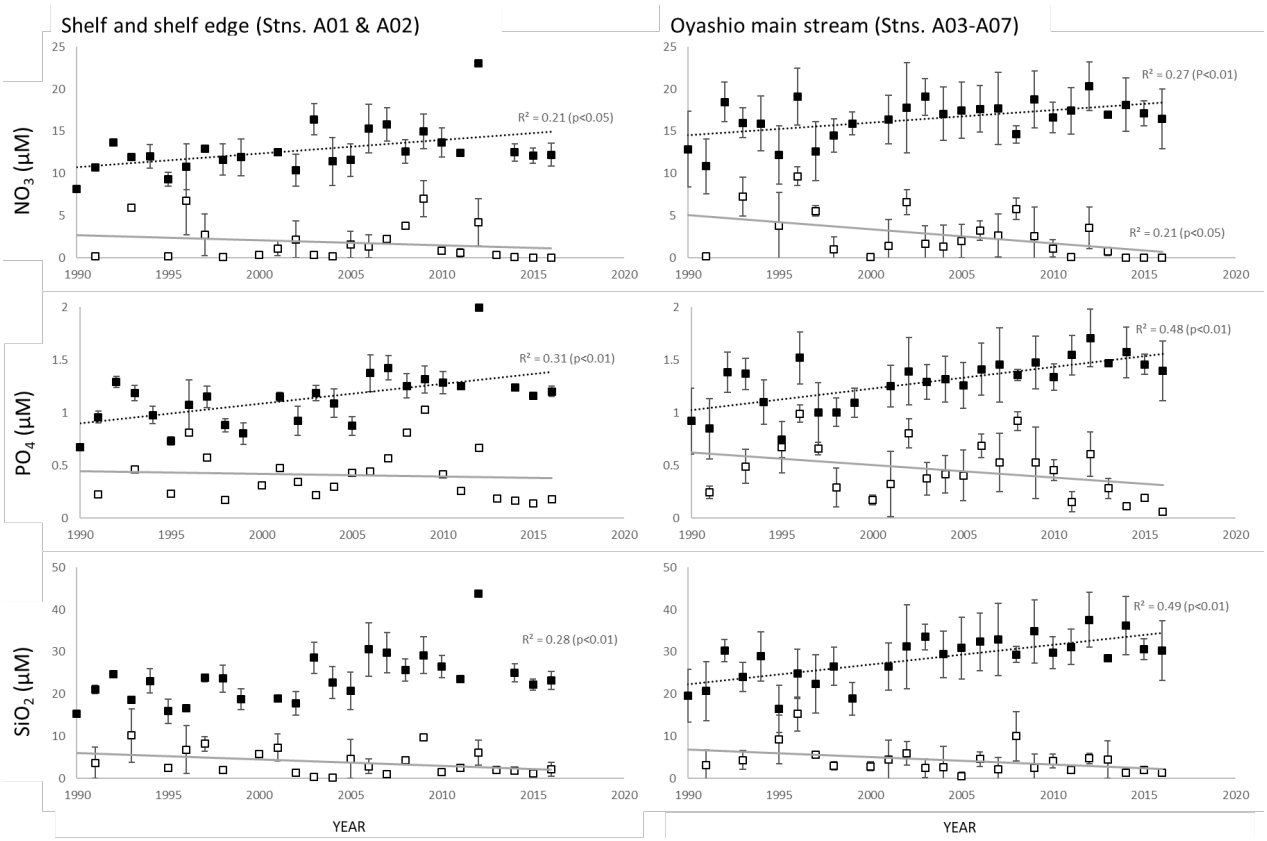

[Figure R18-11] Year-to-year time series of concentrations of nutrients at the sea surface. Solid and open squares denote the monthly means in January and July, respectively. Left and right panels correspond to the shelf to shelf-edge region and the slope region associated with the main stream of the Oyashio, respectively. Upper, middle, and lower panel indicates time series of nitrate, phosphate, and silicate concentrations, respectively. The vertical bars represent mean ± one standard deviation. Regression lines in each panel indicate linear trends estimated by the least square method. Regarding a significant trend ($p < 0.05$), its determination coefficient and criterion of p-value are illustrated.

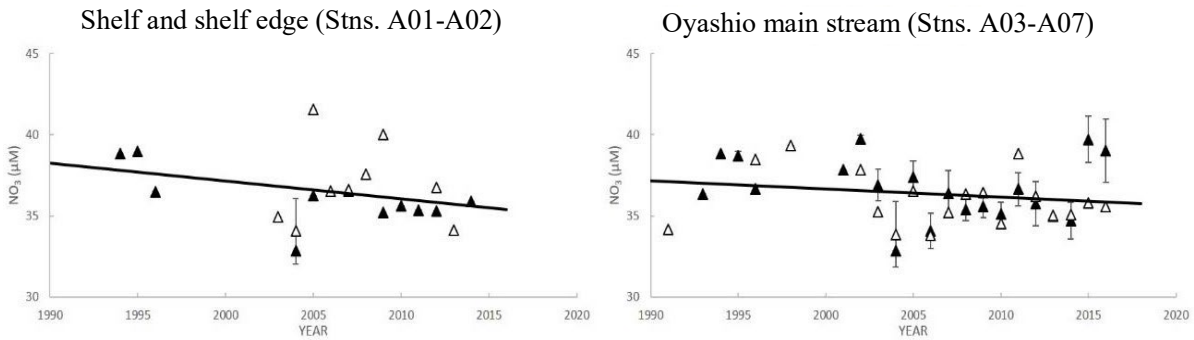

[Figure R18-12] Same as upper panels in Figure R18-11, but for an isopycnal layer with 26.8–26.9 σ_t. Linear trends, which were estimated from monthly means both for January and July after 1990, are not significant under the 95-% confidence interval

5.2. Dissolved Oxygen

5.2.1. Deoxygenation

(Sasano)

Over the past several decades, the decrease of dissolved oxygen (O_2) has been observed in the western North Pacific (Keeling et al. 2010, and references therein). Together with the warming and acidification of the ocean that are occurring concurrently, the trend toward dissolved O_2 decline (i.e., ocean deoxygenation) is considered as one of the serious consequences of climate change on the marine environment driven by human activities (Gruber 2011).

The Oyashio is the western boundary current of the Western Subarctic Gyre in the North Pacific that reaches off the eastern coast of northern Japan. In the Oyashio, significant trends toward decreasing O_2 have been found on isopycnal surfaces between σ_θ = 26.6 and 27.5 kg m^{-3} (Figure R18-13; modified from Sasano et al. (2018)). The highest rate of O_2 decrease (-0.70 ± 0.06 μmol kg^{-1} yr^{-1}) has been determined on σ_θ = 26.7 kg m^{-3} in the subsurface temperature-minimum (dichothermal) layer. Sasano et al. (2018) suggested that vertical exchanges of water in the upper layers of the subarctic North Pacific have diminished, and thereby the O_2 content in the subsurface has been reduced. Additionally, because the Oyashio water itself has its sources in the Okhotsk Sea Mode Water (OSMW) and in Western Subarctic water (WSAW), changes in the O_2 concentration in the Oyashio region are also attributable to the changes in those in the source region (Andreev and Kusakabe 2001; Nakanowatari et al. 2007).

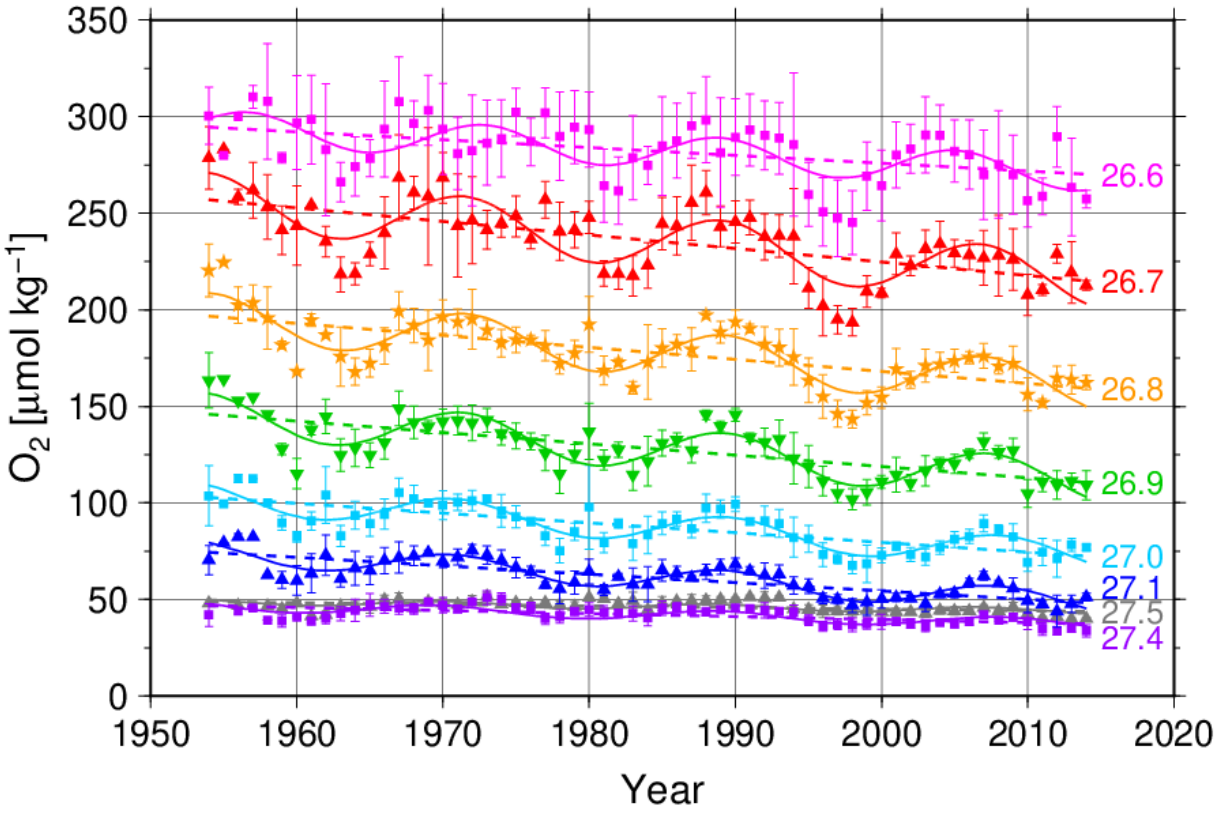

[Figure R18-13] Time series of O_2 on isopycnals from σ_θ = 26.6 to 27.5 kg m^{-3} in the Oyashio region. Thick broken and solid lines indicate trends and oscillations. Error bars indicate standard deviations in each year. Modified from Sasano et al. (2018).

Superimposed on the secular trend of O_2 decline, O_2 concentration has been oscillating in the bidecadal time-scale (Figure R18-13). Because the oscillations of O_2 are well-correlated with North Pacific Index (Trenberth and Hurrell 1994), they are considered to be linked with the changes in atmospheric forcings (Ono et al. 2001) through the subsequent oscillations in the mixing ratio of OSMW and WSAW that have different O_2 concentrations (Takatani et al. 2012; Sasano et al. 2018). They are also attributable to the 18.6-year period nodal tidal cycle which induces tidal diapycnal mixing around the Bussol' Strait in the Kuril Islands (Osafune and Yasuda 2006). However, the controlling mechanisms for the bidecadal oscillations are not yet fully understood to date.

Monitoring the changes in the physical and biogeochemical variables such as O_2 for the extended period is a key to understand the linkage between decadal to longer-term variations in the circulations of the atmosphere and the ocean and their impacts on the O_2 content of the ocean. Clarifying the changes in O_2 in the OSMW and in the WSAW, respectively, are also very important to understand the cause of long-term O_2 decrease in the Oyashio and the subarctic North Pacific in more detail.

5.2.2. Potential impacts on organisms in continental margins

(Ono)

The O_2 concentration in Region 18 has been monitored intensively mainly by the Japan Meteorological Agency, and temporal variation of O_2 content in open ocean area was analysed using these data. Multi-decadal decrease of O_2 was detected in subsurface waters and were described in Section 5.2.1. Fortunately, level of O_2 in continental shelf waters is still high enough for most marine organisms (ca., > 5.5 ml/L at 200 m), and severe biological affection by deoxygenation has not been reported in Region 18.

However, in continental slope area, shoaling trend of hypoxia boundary (O_2 = 1.4 ml/L) has been detected by recent analysis (Ono et al. 2011). In the continental slope area off the Hokkaido coast, the O_2 concentration at a fixed depth from 300 m to 1000 m had been decreased at the rate of −0.06 to −0.07 ml/L/decade. As this result, the hypoxia boundary shoaled from 680 m in 1951 to 560 m in 2010 (Figure R18-14). The deepest catch of Pacific cod occurred at 720 m in 1957 and at 575 m in the 2000s (Figure R18-15). Although there are many factors controlling deepest catch depth, resemblance of hypoxia boundary depth and deepest catch depth indicate us that hypoxia may be one of the main factors that determine deepest habitat of Pacific cod in this area. Recent studies showed that fishes are affected by O_2 concentration even in higher level than "lethal boundary" or "escape boundary" (sublethal hypoxia). If we assume "sublethal hypoxia boundary" as the level of O_2= 3.5 ml/L (Vaquer-Sunyer and Duarte 2008), this boundary becomes 359 m in 1951 and 321 m at 2010, respectively (Figure R18-14). This result indicates that many demersal species in continental slope area other than Pacific cod may have been received sublethal level of hypoxic stresses.

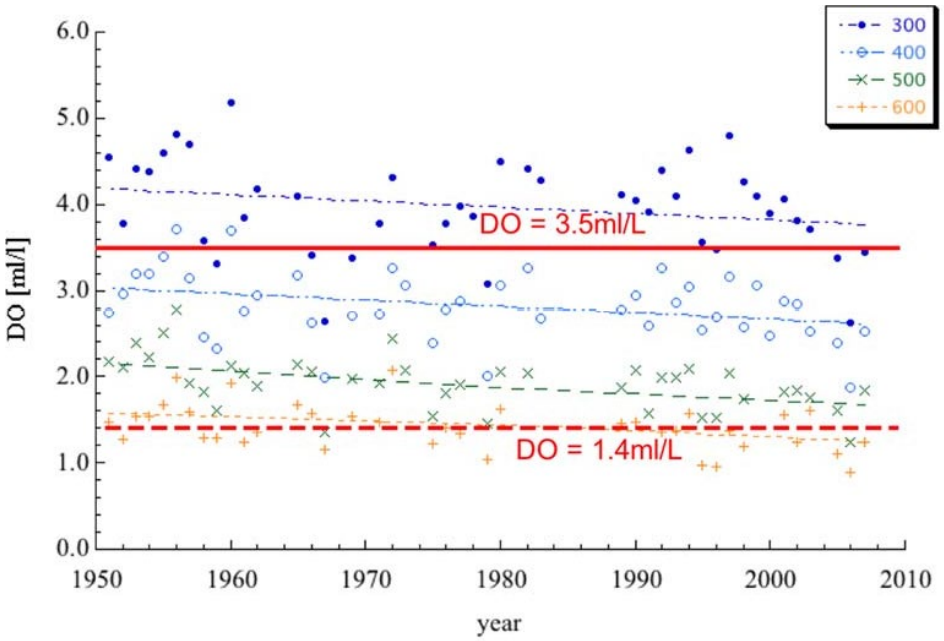

[Figure R18-14] Temporal variation of oxygen concentration on several isobaths from 300 m to 600 m in the continental slope area off the Hokkaido coast. Red dashed and solid lines show levels of DO = 1.4 ml/L and DO = 3.5 ml/L, respectively, which corresponds to average escape boundary and sublethal hypoxia boundary, respectively, of fishes (Renaud 1986).

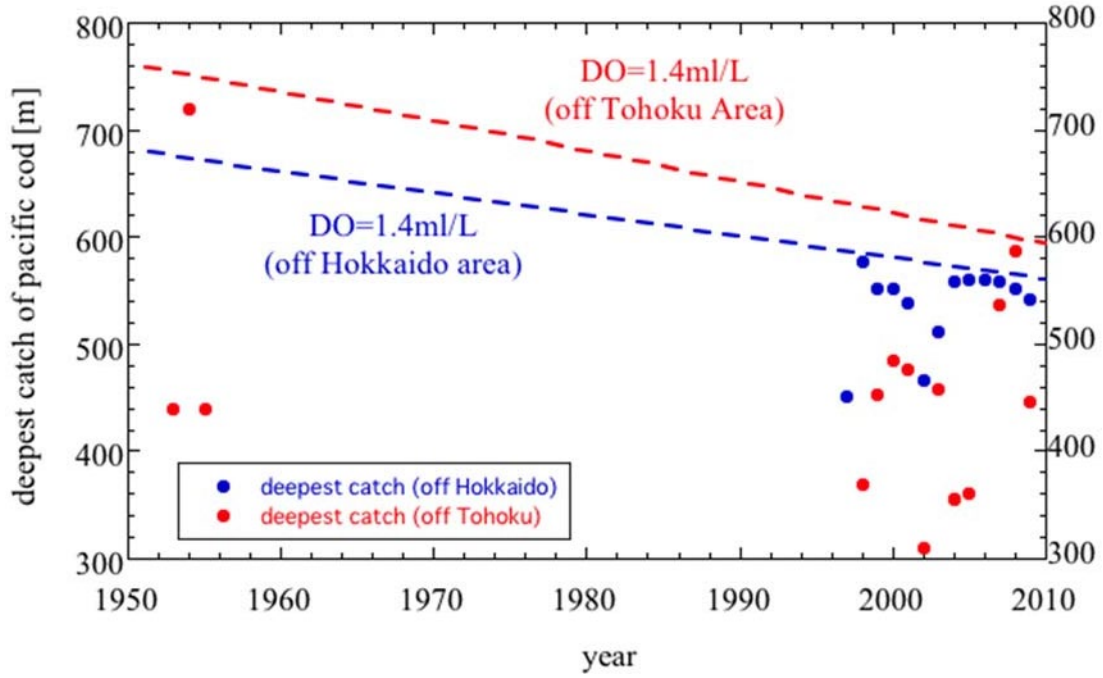

[Figure R18-15] Temporal variation of deepest catch depth of Pacific cod obtained by test operations of the Japan Fisheries Agency in the areas of Tohoku Prefecture (blue dots) and Hokkaido Prefecture (red dots). Blue and Red dashed lines represent depth of hypoxia boundary (DO = 1.4 ml/L) in off-Hokkaido area and off-Tohoku area, respectively.

5.3 Anthropogenic radionuclides

(Kaeriyama)

After the Fukushima Dai-ichi nuclear power plant accident occurred in March 2011, anthropogenic radionuclides such as iodine-131, cesium-134, and -137 (^{131}I, ^{134}Cs and ^{137}Cs), were released into the ocean through atmospheric deposition and as direct releases (Chino et al. 2011; Buesseler et al. 2011). The evaluation of ^{134}Cs and ^{137}Cs in the marine environment is important for addressing risks to both marine ecosystems and public health through consumption of fisheries products, because of their long half-life (2.07 years for ^{134}Cs and 30.07 years for ^{137}Cs). Before this accident, radioactive Cs also existed in the North Pacific. Most of this material originated via global fallout as a result of nuclear weapons testing held during the 1950s and 1980s (Aakrog 2003; Bowen et al. 1980). After this era of global fallout, the concentration of ^{137}Cs in the surface seawater has decreased with time and the horizontal distribution of ^{137}Cs in surface seawater has been relatively homogenous over the entire North Pacific in the 2000s (Aarkrog 2003; Hirose and Aoyama 2003; Hong et al. 2004). In the 2000s, the ^{137}Cs concentration in the surface water was almost at a level of 1.5–2.0 Bq m^{-3} (Hirose and Aoyama 2003; Povinec et al. 2004).

In a short period of time the Fukushima-derived radiocesium (^{134}Cs and ^{137}Cs) spread broadly in the surface water especially in the north area of Kuroshio Extension, because the Fukushima Dai-ichi nuclear power plant is located at 37˚25'N, 141˚02'E north of the Kuroshio Extension (Aoyama et al. 2013; Kaeriyama et al. 2013; Kumamoto et al. 2015; Smith et al. 2014) (Figure R18-16). Some part of these Fukushima-derived radiocesium had been trapped in the mode waters (Subtropical Mode Water and Central Mode Water), and transported to the subtropical area south of the Kuroshio Extension (Aoyama et al. 2016; Kaeriyama et al. 2014; 2016; Kumamoto et al. 2014; Men et al. 2015; Yoshida et al. 2015).

After the Fukushima accident, the concentration of ^{137}Cs in surface seawater in the Oyashio region has been monitored since June 2011 by FRA (Kaeriyama 2015; 2017). In June 2011, the concentration of ^{137}Cs in surface water was 14±3.9 Bq m^{-3}, higher than those just before the Fukushima accident (~ 2.0 Bq m^{-3}) (Figure R18-17). The concentration of ^{137}Cs increased up to 70±4.2 Bq m^{-3} in September 2011, then rapidly decreased until May 2012. The increase of ^{137}Cs in the Oyashio water observed during the first year from the accident seems to have originated from the atmospheric deposition occurred during March and April 2011 in the western and central North Pacific (cf. Honda et al. 2012; Kobayashi et al. 2013). In May 2012, 15 months after the Fukushima accident, the concentration of ^{137}Cs were in the range of 2.0–4.6 Bq m^{-3}, slightly higher than the concentration level observed before the accident (~ 2.0 Bq m^{-3}). After that, the concentration of ^{137}Cs were almost constant until May 2017 (1.7±0.44 Bq m^{-3}; n=14) and this average value is mostly equal to the background level of ^{137}Cs in the surface water in the North Pacific before the Fukushima accident.

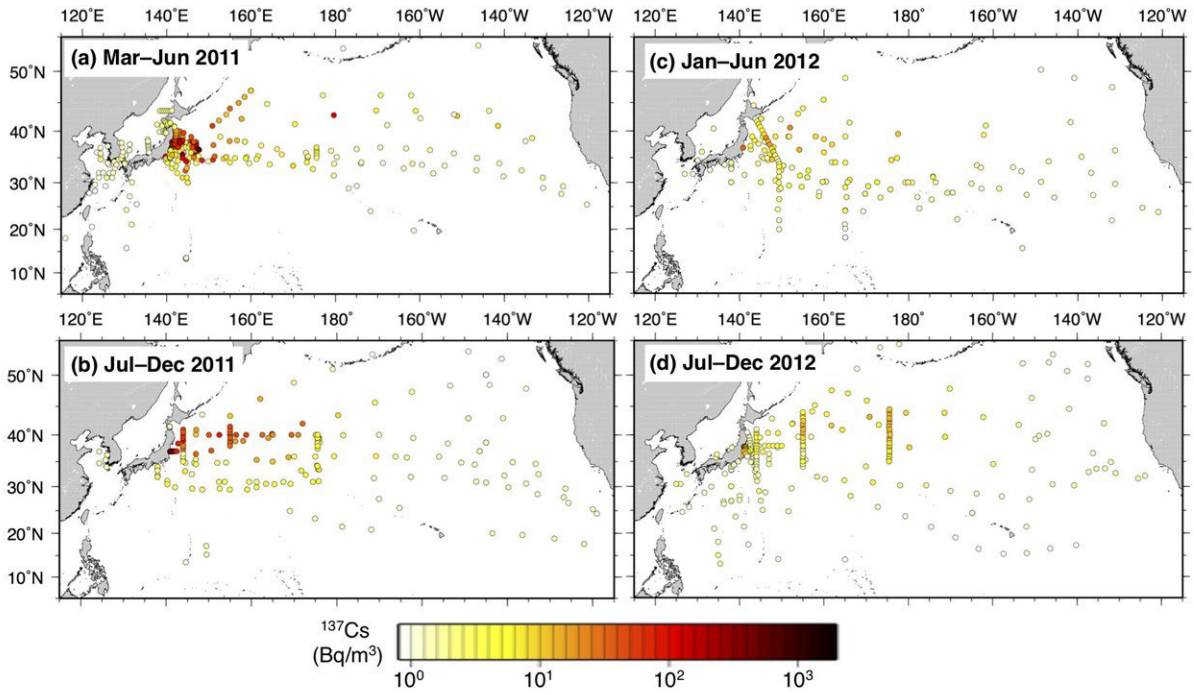

[Figure R18-16] The concentration of ^{137}Cs in the surface seawater in the North Pacific and adjacent seas: (a) obtained during March–June 2011, (b) during July–December 2011, (c) during January–June 2012 and (d) during July–December 2012. The color of the closed circles indicates the concentration of ^{137}Cs. Modified from Kaeriyama (2017).

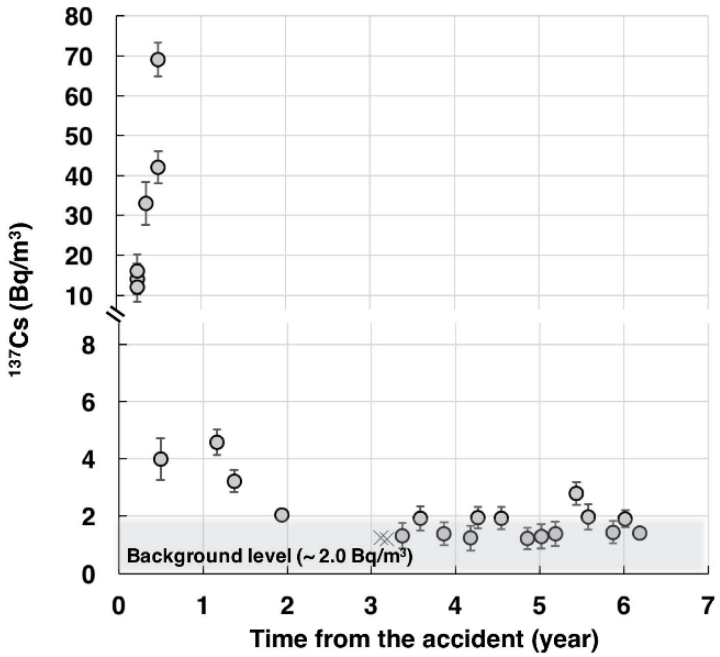

[Figure R18-17] Temporal changes in the concentration of ^{137}Cs in surface water collected in the Oyashio region. Error bars indicate counting error (±1σ). When ^{137}Cs was under detection limit (< 3σ), the detection limit was plotted as cross symbols. Grey area indicates background level of ^{137}Cs concentration in the North Pacific

6. Phytoplankton

(Taniuchi)

The Oyashio region is known to be a high productivity region of the world's oceans. In this region, the abundance of phytoplankton exhibits drastic seasonal variation. The pattern of seasonal variation of chlorophyll *a* (hereafter, Chl. *a*) concentration was reported based on of the A-line monitoring dataset from 1990 to 2002 (Saito et al 2002; Kasai and Ono 2007). After 2002, the pattern of seasonal variation in the Oyashio region hardly seemed to change (Figure R18-18). The concentration of Chl. *a* was minimum in winter (January) and increased to the maximum (> 4 μg/L) in spring (May). The concentration of Chl. *a* decreased to around 1 μg/L in summer (July). The concentration of Chl. *a* increased slightly in autumn (October).

Section 5.1 in this report reported the interdecadal increase of nutrient concentrations in January in the Oyashio region on the slope. As well as the nutrient concentrations, the concentration of Chl. *a* in January showed an interdecadal increase for the recent 25 years (Figure R18-19, $p<0.05$). It is likely that the increase of nutrient concentrations enhanced the phytoplankton growth. In October, the concentration of Chl. *a* tended to increase until 2009 and decrease after 2010 (Figure R18-19). Significant trends of concentration of Chl. *a* were not apparent in the other seasons than January.

Generally, phytoplankton is composed from many kinds of algae, the size, shape and characteristics of which are different. Odate and Maita (1988) studied the distribution of size composition of Chl. *a* in western North Pacific in spring. Their study showed that dominant phytoplankton size in the subarctic region was >10 μm, whereas that in the Kuroshio-Oyashio Transitional Zone and subtropical region was <2 μm. It is worth noting that dominant phytoplankton size changes on a seasonal timescale. For example, during summer, the dominant fraction in the Oyashio region is limited to the small size <2 μm (Hayakawa et al. 2008).

Concentration of size fractionated Chl. *a* on the A-line started to be measured from 2007 (Figure R18-20). The size component >10 μm to total Chl. *a* increased from an early spring (March) and reached more than 50 % in spring (May), as reported by Odate and Maita (1988). The <2 μm fraction increased from summer (July), became the most dominant (> 50 %) in autumn (October), and decreased to 30−50 % in winter (January). In the Oyashio region, the large fraction of >10 μm was frequently highlighted due to major composition of phytoplankton in spring bloom, but the fraction of <2 μm is dominant in all seasons except the spring.

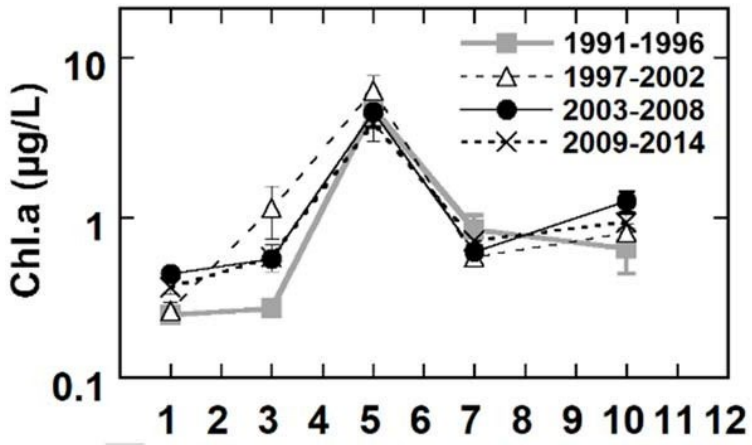

[Figure R18-18] Monthly mean of Chl. *a* concentration at the sea surface in the Oyashio region (Stns. A03–A07) that was averaged for four periods such as 1991–1996, 1997–2002, 2003–2008, and 2009–2014. Vertical bar represents standard error that was estimated from the dataset of 1991–2014.

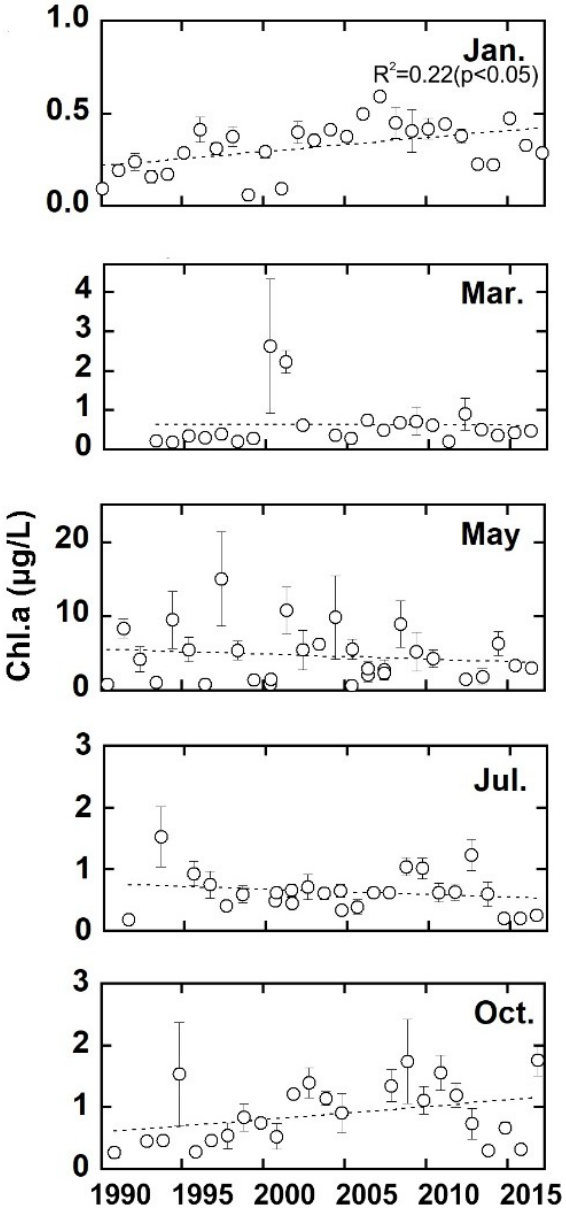

[Figure R18-19] Year-to-year time series of concentration of Chl. *a* at the sea surface in the Oyashio region (Stns. A03–A07) for individual months. Panels from the top to bottom correspond to January, March, May, July, and October. The regression line only for January is significant at the 95 % confidence limit.

In general, picoeukaryotes and *Synechococcus* sp. were considered to be the major groups of the < 2 µm size fraction. In the Oyashio region, the cell density of picoeukaryotes showed little seasonal variation (Figure R18-21); it was minimum (c.a. 3000 cell/L) in winter (January) and increased gradually to maximum (c.a. 10000 cells/L) in autumn (October). On the other hand, the cell density of *Synechococcus* sp. showed a distinct seasonal variation (Figure R18-21); it was minimum (500 cells/L) in spring (May) and then increased to more than 10000 cell/L in summer (July). High cell density was restricted to autumn (October). The increase of cell density in summer and autumn corresponded to the dominance of <2 µm fraction of Chl. *a*. These results suggested that *Synechococcus* sp. determined the abundance of <2 µm fraction of Chl. *a* during summer to autumn.

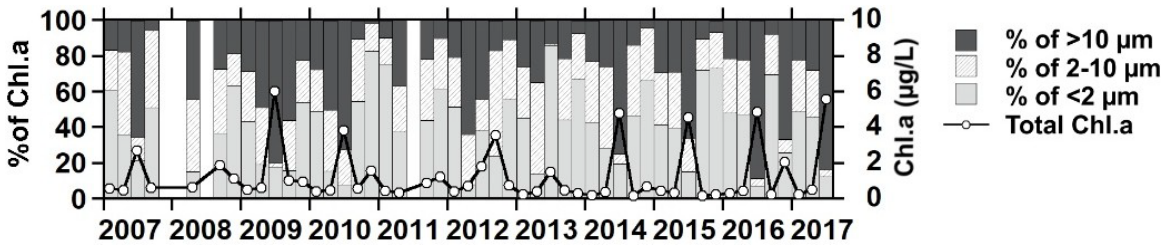

[Figure R18-20] Time series of size composition of Chl. *a* at the depth of 10 m in the Oyashio region (Stns. A03–A07). Total Chl. *a* concentration for each month is depicted by thick lines with open circles.

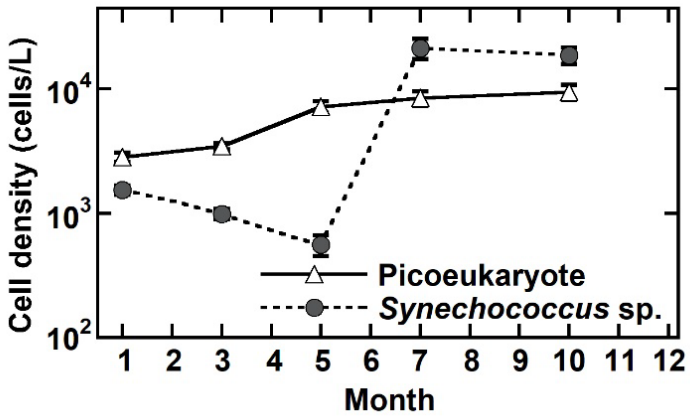

[Figure R18-21] Monthly mean of cell density of picoeukaryotes and *Synechococcus* sp. at the depth of 10 m in the Oyashio region (Stns. A03–A07). The monthly mean was estimated from dataset from 2003– 2014. The vertical bars represent one? standard error estimated from the dataset from 2003–2014.

7. Zooplankton

7.1. Mesozooplankton

(Tadokoro)

Oyashio and Kuroshio-Oyashio Transition waters are important feeding and nursery areas for the pelagic fishes which are commercially important in Japan. Those fishes mainly feed on mesozooplankton. Therefore, the variation of mesozooplankton is considered to be a cause of the population dynamics of those fishes (e.g., Watanabe et al. 1996). Decadal scale variation of the mesozooplankton was well studied in the Odate Project and revealed the relationship with climatic regime shift (Chiba et al. 2006, 2008, 2009), variation in feeding pressure of Japanese sardine (Tadokoro et al. 2005) and the18.6 year cycle of the strength of diurnal tide (Tadokoro et al. 2009). However the period of those studies covered from 1960 to end of 1990. The recent variation of the mesozooplankton from 2000 to present have not been reported until now. We analyzed the mesozooplankton samples obtained at a monitoring transect of the A-line conducted by Fisheries Resources Institute (Kushiro and Shiogama) in the Oyashio and Kuroshio-Oyashio Transition waters and revealed the geographical, seasonal and interannual variation of mesozooplankton community structure from 2007 to 2017. Observations have been carried out five times each year (January, March, May, July, and October) along the A-line transect (Figure R18-9). Mesozooplankton samples were collected by vertical haul of NORPAC net (mouth diameter: 45 cm, total length: 180 cm, mesh size: 0.335 mm) from 150 m or sea floor to 0 m at 17 stations along the A-line. The total number of collected samples collected was 748. Samples were immediately preserved in 5 % buffered formalin. The number of individuals for each species were counted under the microscope. Target taxonomic groups are, Copepoda, Chordata, Amphipoda, Euphausiacea, Cnidaria, Chaetognatha, Gastropod, and Diplostraca. To classify the mesozooplankton community based on the species composition, cluster analysis was used. The variable is the individual count of each species and the value is transformed by the common logarithm. Bray-Curtis and Ward methods are used for similarity index and distance, respectively.

354 species appeared in this area including 205 Copepoda, 35 Chordata, 34 Amphipoda, 25 Euphausiacea, 22 Cnidaria, 19 Chaetognatha, 8 Gastropoda, and 6 Diplostraca.

The cluster analysis identified four community groups (Figure R18-22). The top 10 abundant species in each group are indicated in Table R18-1. Cold water Copepoda mainly appeared in groups 1 and 2. In those groups, species such as *Neocalanus plumchrus* which appeared from spring to summer mainly composed the group 2. On the other hand, species such as *N. flemingeri* which appeared from winter to spring mainly composed the group 1. It is considered that although the two are cold water communities, seasonality is different. We therefore named the group 1 Cold winter-spring community and group 2 Cold spring -summer community. Group 3 was composed by cold and warm species and we named it Transition community. Group 4 was mainly composed by warm species and we named it Warm community.

Table R18-1

Most abundant top 10 species and species number of each groups. The species indicated by blue and red character are cold and warm species, respectively.

	Group 1 Cold winter-spring community	Nx1000 m^2	Group 2 Cold spring-summer community	Nx1000 m^2	Group 3 Transition community	Nx1000 m^2	Group 4 Warm community	Nx1000 m^2
1	*Pseudocalanus newmani*	4.9	*Pseudocalanus newmani*	4.4	*Doliolum nationalis*	2.6	*Penilia avirostris*	2.6
2	*Metridia pacifica*	1.8	*Oithona similis*	3.0	*Pseudocalanus newmani*	2.4	*Doliolum denticulatum*	2.0
3	*Pseudocalanus minutus*	0.8	*Eucalanus bungii*	2.2	*Oikopleura longicauda*	1.4	*Doliolum nationalis*	1.7
4	*Oithona similis*	0.5	*Neocalanus plumchrus*	1.7	*Oithona atlantica*	1.4	*Ctenocalanus vanus*	1.6
5	*Neocalanus flemingeri*	0.4	*Metridia pacifica*	1.4	*Metridia pacifica*	1.1	*Oikopleura longicauda*	1.0
6	*Neocalanus cristatus*	0.4	*Pseudocalanus minutus*	1.2	*Ctenocalanus vanus*	1.1	*Ditrichocorycaeus affinis*	0.7
7	*Acartia (Acartiura) longiremis*	0.2	*Fritillaria borealis f.typica*	1.2	*Ditrichocorycaeus affinis*	1.0	*Clausocalanus furcatus*	0.6
8	*Oikopleura labradoriensis*	0.2	*Eukrohnia hamata*	0.6	*Paracalanus parvus*	1.0	*Clausocalanus parapergens*	0.6
9	*Neocalanus plumchrus*	0.1	*Neocalanus flemingeri*	0.5	*Dolioletta gegenbauri*	0.8	*Oithona atlantica*	0.5
10	*Scolecithricella minor*	0.1	*Oikopleura labradoriensis*	0.5	*Muggiaea atlantica*	0.7	*Paracalanus parvus*	0.4
	Others	0.8	Others	4.2	Others	10.1	Others	12.0
	Total	10.1		21.0		23.6		23.7
	Biomass (wet weight g m-2)	8.4		17.6		8.7		4.7
	Species Number	46		77		144		245

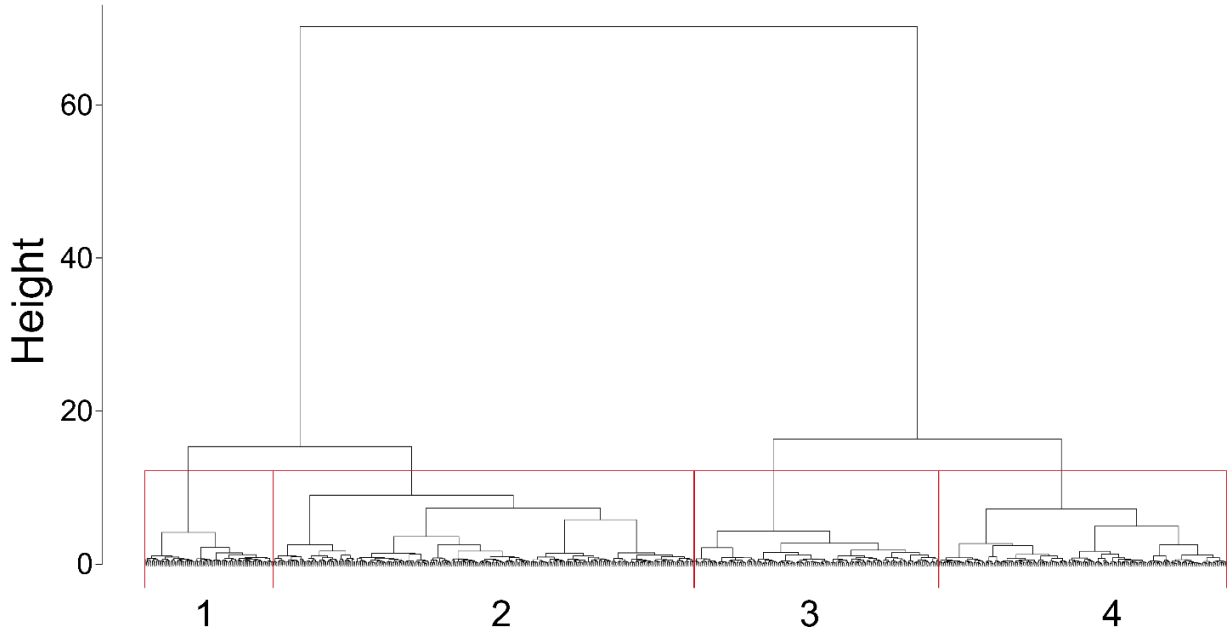

[Figure R18-22] Dendrogram of the cluster analysis for the species level abundance of each sampling station. We classified mesozooplankton community into 4 groups.

Next, we examined the relationships between community structure and water mass, which is classified by temperature and salinity at 100-m depth on the basis of water-mass definition of Hanawa and Mitsudera (1987) (Figure R18-23). The stations were belonged to six water mass of Coastal Oyashio, Surface Coastal Oyashio, Oyashio, Surface Oyashio, Kuroshio-Oyashio Transition, and Kuroshio waters. Almost all of the Cold winter-spring community and the Cold spring-summer community appeared in the Oyashio and Coastal Oyashio waters. The Transition community mainly appeared in Oyashio and Kuroshio-Oyashio Transition waters. The Warm community mainly appeared in the Kuroshio-Oyashio Transition and Kuroshio waters. These results indicate that the mesozooplankton community structure and water mass are tight linked with each other.

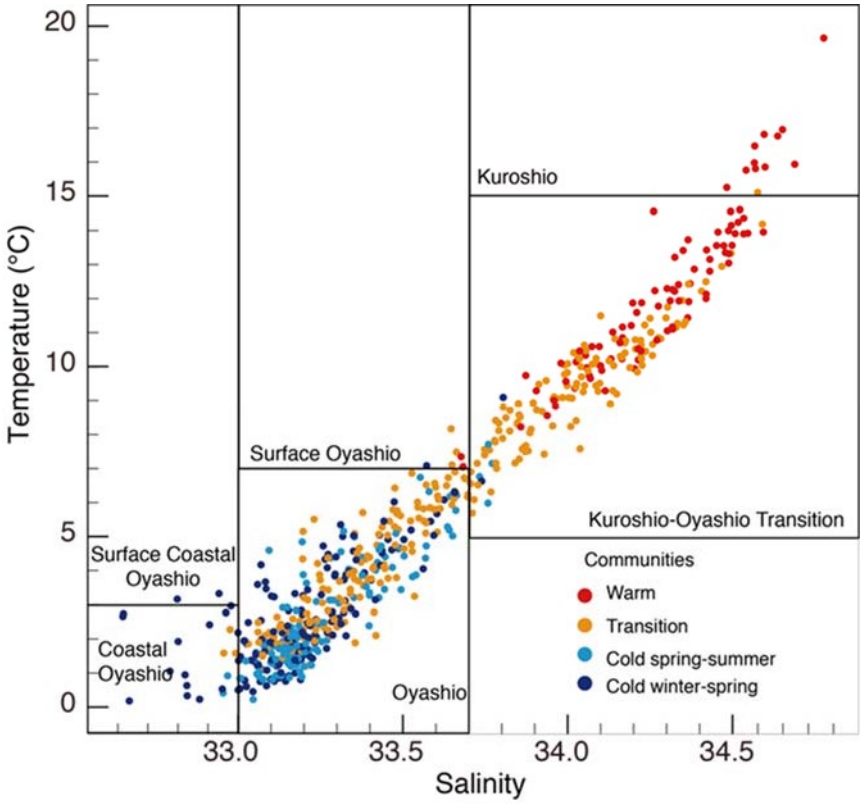

[Figure R18-23] Water temperature (°C) and salinity at 100m depth that each group appeared. Classification of water mass was referred by Hanawa and Mitsudera (1987).

From January to March, Cold winter-spring community mainly appeared, however Cold spring-summer community also appeared in 2007–2009 and 2014 in the northern areas (Figure R18-24). Transition community mainly appeared in the southern areas and the Warm community also appeared in the most southern areas except for in 2011–2013.

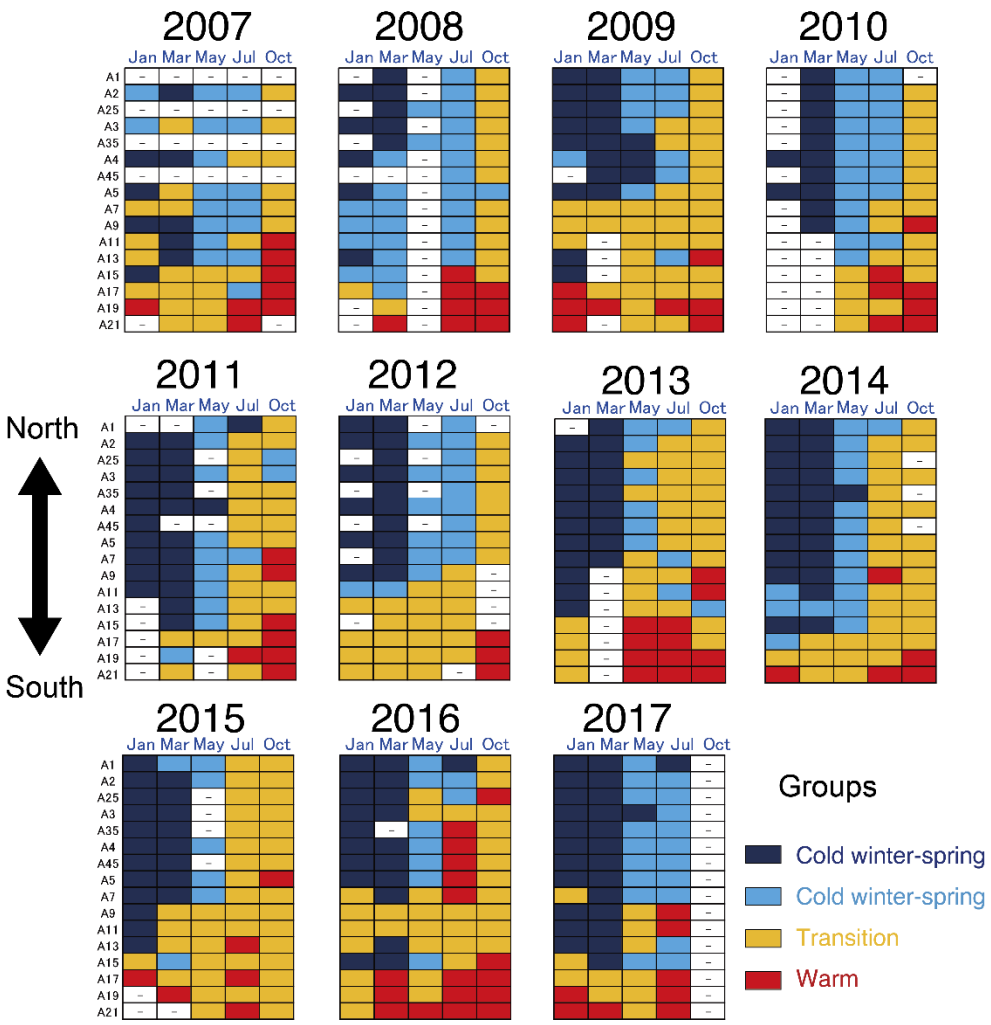

[Figure R18-24] The groups that appeared in each month and each station from 2007 to 2017.

In May, the Cold spring-summer community mainly appeared and Cold winter-spring community only appeared in 2009–2011, 2014, and 2017. The Transition community mainly appeared in the southern areas and the Warm community also appeared in the most southern areas in 2013 and 2016.

In July, Cold spring-summer community mainly appeared in 2007–2010, and 2012 in the northern areas. During this period, the Transition community mainly appeared in the southern areas, and Warm community appeared in the most southern areas. On the other hand, Transition community mainly appeared in 2011, and 2013–2015 in the northern areas. Moreover, the Warm community occupied wide areas in the northern areas. However, the Cold spring-summer community mainly appeared in the northern to southern areas and Warm community only appeared in the most southern areas.

In October, the Transition community dominated the northern areas and Warm community appeared in the southern areas throughout the observation.

Based on the results, schematic of the seasonal variation of the mesozooplankton community can be indicated as follows. From January to March, the Cold winter-spring community appears in the northern areas and the Transition community appears in the southern areas, and the Warm community appears in the most southern areas. In May, the Cold spring-summer community mainly appeared in the northern areas, the Transition community appears in the southern areas, and the Warm community appears in the most southern areas.

In July, the Cold spring-summer community or the Transition community appeared in the northern areas, and Warm community appears in the most southern areas. In October, the Transition community almost only appeared in the northern areas and the Warm community appeared in the southern areas. This study also revealed that year to year variation of the seasonal pattern of the community structure. Appearance of the communities corresponded with the water mass features (Figure R18-23). Therefore, the year to year variation of the seasonal pattern of the community structure is considered to be related to the variation of the water mass. For example, the area of the Transition community and the Warm community expanded to the northern areas in July and October from 2015 to 2016. In those years, saline and high temperature waters also expanded to the northern areas (Figure R18-25).

(a): salinity

2007

	Jan	Mar	May	Jul	Oct
A1	–	–	–	–	–
A2	33.1	33.5	33.2	33.2	33.2
A25	–	–	–	–	–
A3	33.1	33.6	33.3	33.2	33.3
A35	–	–	–	–	–
A4	33.2	33.6	33.3	33.7	33.3
A45	–	–	–	–	–
A5	33.5	33.6	33.5	33.2	33.8
A7	33.8	33.7	33.2	33.2	33.7
A9	33.8	33.3	33.6	33.3	33.1
A11	33.5	33.1	33.7	33.4	34.4
A13	33.8	33.2	33.7	33.4	34.2
A15	33.3	34.2	33.7	33.2	34.2
A17	34.0	34.2	34.3	33.2	34.5
A19	34.4	34.5	34.3	34.5	34.5
A21	34.4	34.4	34.5	34.8	34.4

2008

	Jan	Mar	May	Jul	Oct
A1	–	–	–	–	–
A2	32.8	33.1	33.5	33.3	–
A25	–	–	–	–	–
A3	33.1	33.3	33.4	33.3	33.4
A35	–	–	–	–	33.4
A4	33.2	33.2	33.6	33.5	33.4
A45	–	–	–	–	33.5
A5	33.2	33.4	33.6	33.5	–
A7	33.4	33.6	33.2	33.5	33.4
A9	33.4	33.2	33.4	33.7	33.3
A11	33.3	33.4	33.2	33.4	33.3
A13	33.6	33.8	33.3	33.4	33.5
A15	33.4	33.6	33.6	34.4	33.5
A17	33.9	33.6	34.4	34.4	34.2
A19	–	33.9	34.3	34.5	34.3
A21	–	34.5	34.4	34.5	34.2

2009

	Jan	Mar	May	Jul	Oct
A1	–	–	–	–	–
A2	33.2	33.1	33.2	33.2	33.2
A25	33.2	–	33.2	–	–
A3	33.3	33.1	33.2	33.5	33.3
A35	33.2	–	33.1	–	–
A4	33.2	33.2	33.2	33.2	33.4
A45	33.2	–	33.2	–	–
A5	33.3	33.2	33.1	33.7	33.3
A7	34.0	33.7	34.2	33.7	33.2
A9	34.1	34.0	34.2	33.6	33.2
A11	34.0	–	34.0	33.2	33.7
A13	33.7	–	33.6	33.2	34.1
A15	33.3	33.4	34.1	33.1	33.4
A17	34.5	34.4	33.9	33.6	33.6
A19	34.6	34.5	33.9	34.1	34.2
A21	34.5	34.4	34.2	33.5	34.5

2010

	Jan	Mar	May	Jul	Oct
A1	–	–	–	–	–
A2	33.2	33.1	33.1	33.1	33.2
A25	–	–	–	–	33.2
A3	33.8	33.1	33.1	33.1	33.2
A35	–	–	–	–	33.2
A4	33.6	33.1	33.1	33.2	33.2
A45	–	–	–	–	33.2
A5	33.4	33.1	33.1	33.1	33.2
A7	33.5	32.8	33.2	33.7	33.3
A9	33.6	33.5	33.1	33.5	34.1
A11	33.2	–	33.1	33.2	34.0
A13	33.4	–	33.2	33.5	33.2
A15	34.3	–	33.4	34.2	33.6
A17	33.9	–	34.3	34.5	34.3
A19	33.9	–	34.2	34.0	34.4
A21	33.6	–	34.1	34.6	34.3

North

ST

South

2011

	Jan	Mar	May	Jul	Oct
A1	–	–	–	–	–
A2	33.2	33.2	33.2	33.1	33.2
A25	33.3	33.2	–	33.4	33.3
A3	33.3	33.2	33.2	33.2	33.3
A35	33.3	33.1	–	33.0	33.2
A4	33.3	33.2	33.2	33.6	33.2
A45	33.3	33.4	–	33.5	33.5
A5	33.3	33.4	33.2	33.1	33.9
A7	33.2	33.6	33.2	33.1	34.1
A9	33.2	33.2	33.1	33.7	34.1
A11	33.3	33.0	33.2	33.1	33.2
A13	–	33.2	33.2	33.5	33.6
A15	–	33.4	33.1	33.6	34.3
A17	–	33.4	33.8	34.0	34.2
A19	–	33.3	–	34.1	34.2
A21	–	34.3	–	33.5	34.3

2012

	Jan	Mar	May	Jul	Oct
A1	–	–	–	–	–
A2	33.3	32.9	33.2	33.8	33.6
A25	–	–	–	–	–
A3	33.2	33.1	33.5	33.4	33.4
A35	–	–	–	–	–
A4	33.4	33.2	33.2	33.2	33.2
A45	–	–	–	–	–
A5	33.4	33.2	33.2	33.2	33.4
A7	–	33.1	33.1	33.2	33.7
A9	33.5	33.2	33.6	33.4	34.1
A11	33.3	33.5	33.9	33.3	33.4
A13	33.7	33.6	33.9	33.3	33.3
A15	–	34.3	33.4	33.5	33.3
A17	34.2	34.1	34.1	34.1	34.1
A19	34.2	34.1	34.2	34.2	34.2
A21	34.1	34.2	34.2	34.3	34.2

2013

	Jan	Mar	May	Jul	Oct
A1	–	–	–	–	–
A2	32.9	–	33.0	33.4	33.3
A25	33.0	–	33.4	33.3	33.4
A3	33.2	–	33.4	33.4	33.3
A35	33.4	–	33.3	33.2	33.2
A4	33.3	–	33.7	33.1	33.3
A45	33.4	–	33.4	33.2	33.4
A5	33.2	33.3	33.2	33.2	33.3
A7	33.5	33.3	33.2	33.1	33.3
A9	33.3	–	33.7	33.2	34.5
A11	–	–	33.6	33.1	34.5
A13	–	–	33.8	33.2	33.2
A15	34.1	–	34.4	34.1	33.4
A17	34.0	–	34.3	34.0	33.1
A19	34.0	–	34.4	34.5	33.7
A21	34.0	–	34.4	34.5	34.6

2014

	Jan	Mar	May	Jul	Oct
A1	–	–	–	–	–
A2	33.2	32.7	33.0	33.4	33.5
A25	33.2	33.0	33.0	33.5	–
A3	33.1	33.1	33.2	33.3	33.4
A35	33.1	33.0	33.1	33.3	–
A4	33.2	33.3	33.0	33.1	33.4
A45	33.2	33.0	33.1	33.6	–
A5	33.2	33.1	33.1	33.3	33.3
A7	33.4	33.0	33.4	33.4	33.1
A9	33.1	33.6	33.4	34.1	33.1
A11	33.4	33.7	33.3	33.6	33.1
A13	33.3	33.5	33.4	33.1	33.0
A15	33.3	33.4	33.4	33.0	33.1
A17	33.3	33.7	33.8	33.6	33.2
A19	33.8	34.2	34.3	33.1	34.3
A21	34.5	34.3	34.0	34.6	34.2

2015

	Jan	Mar	May	Jul	Oct
A1	–	–	–	–	–
A2	33.0	32.8	33.1	33.8	33.8
A25	33.0	–	–	33.7	33.6
A3	33.0	33.1	–	33.5	33.5
A35	33.1	–	–	33.5	33.5
A4	33.1	33.1	33.1	33.4	34.2
A45	33.1	–	–	33.4	34.0
A5	33.2	33.1	33.2	33.5	34.0
A7	33.4	33.1	33.2	34.0	34.1
A9	33.3	33.9	33.7	34.0	34.0
A11	33.3	33.8	33.8	33.8	33.6
A13	33.4	33.9	33.6	34.0	33.6
A15	34.2	33.6	34.3	33.9	33.5
A17	34.3	34.1	34.3	34.4	33.7
A19	–	34.4	34.2	34.4	33.4
A21	–	34.4	34.0	34.2	34.1

2016

	Jan	Mar	May	Jul	Oct
A1	–	–	–	–	–
A2	32.9	33.0	33.8	33.2	33.7
A25	–	33.0	33.8	33.6	33.7
A3	33.4	33.0	33.9	33.9	33.7
A35	–	33.0	33.3	34.0	33.4
A4	33.0	33.0	33.0	34.0	33.3
A45	–	33.0	33.0	34.1	33.1
A5	33.0	33.0	33.0	34.1	33.1
A7	33.8	33.1	33.8	34.0	33.3
A9	34.0	34.0	34.0	34.1	33.1
A11	34.0	33.9	34.0	33.0	33.1
A13	33.9	33.3	33.8	33.1	33.3
A15	33.6	33.3	33.1	33.1	33.9
A17	33.9	34.6	33.7	33.9	34.6
A19	34.1	34.5	34.6	34.3	34.7
A21	34.6	34.3	34.5	34.3	34.6

2017

	Jan	Mar	May	Jul	Oct
A1	–	–	–	–	–
A2	32.7	32.8	33.1	33.2	33.2
A25	32.7	33.1	33.1	33.2	33.2
A3	32.8	33.2	33.1	33.1	33.1
A35	33.5	33.1	33.1	33.1	33.3
A4	33.1	33.2	33.1	33.1	33.8
A45	33.1	33.1	33.2	33.1	–
A5	32.9	33.1	33.2	33.2	33.9
A7	34.2	33.1	33.1	33.1	33.4
A9	33.3	33.3	33.8	33.9	33.3
A11	33.1	33.7	34.1	34.0	33.4
A13	33.2	33.2	33.9	33.2	33.1
A15	34.0	33.4	33.2	33.2	33.1
A17	34.1	33.9	34.1	33.9	34.3
A19	34.4	34.3	34.4	34.3	34.3
A21	34.7	34.3	34.4	34.3	34.4

(b): temperature

2007

	Jan	Mar	May	Jul	Oct
A1	–	–	–	–	–
A2	1.9	4.6	1.3	2.2	3.8
A25	–	–	–	–	–
A3	2.0	5.4	2.0	2.3	2.3
A35	–	–	–	–	–
A4	2.4	5.7	2.6	6.2	2.1
A45	–	–	–	–	–
A5	4.9	6.2	4.7	2.1	6.3
A7	8.4	6.7	1.2	2.0	7.0
A9	9.1	2.8	6.2	2.2	2.2
A11	6.9	1.3	6.8	3.6	12.4
A13	7.9	0.9	6.2	3.2	11.2
A15	5.0	10.7	6.6	1.9	11.6
A17	10.0	10.8	11.2	2.0	13.6
A19	13.7	13.0	11.3	13.9	14.4
A21	–	12.2	13.3	19.7	–

2008

	Jan	Mar	May	Jul	Oct
A1	–	–	–	–	–
A2	1.9	0.8	–	1.9	3.6
A25	–	–	8.4	–	2.8
A3	2.5	1.7	–	2.4	2.1
A35	–	–	1.2	–	3.2
A4	2.8	1.6	–	3.9	1.9
A45	–	–	–	–	2.6
A5	2.7	3.2	–	3.8	5.1
A7	4.0	4.4	–	3.4	2.6
A9	4.4	1.5	–	5.0	2.4
A11	4.4	3.4	–	2.4	3.8
A13	3.2	6.0	–	3.2	3.8
A15	4.2	5.2	–	11.4	10.2
A17	7.4	4.7	–	12.0	11.1
A19	–	7.4	–	13.0	9.9
A21	–	13.9	–	13.3	3.7

2009

	Jan	Mar	May	Jul	Oct
A1	–	–	–	–	–
A2	2.5	1.1	1.2	2.1	5.9
A25	2.5	–	1.2	4.2	8.1
A3	2.6	1.2	1.2	4.6	2.9
A35	2.6	–	1.6	5.0	1.9
A4	2.3	1.4	1.6	2.1	2.0
A45	–	–	1.6	2.1	2.4
A5	2.7	1.5	1.5	6.2	3.2
A7	8.4	6.1	10.2	5.7	2.6
A9	8.9	7.6	9.8	5.1	3.1
A11	8.2	–	8.3	2.0	8.8
A13	6.6	–	5.9	1.7	9.3
A15	3.8	–	9.3	2.1	4.2
A17	15.3	12.5	7.3	6.2	5.8
A19	16.0	13.4	7.5	10.2	11.2
A21	15.8	–	10.6	5.5	14.3

2010

	Jan	Mar	May	Jul	Oct
A1	–	–	–	–	–
A2	–	0.6	0.8	1.8	5.1
A25	–	–	–	–	4.3
A3	–	0.8	1.4	0.9	2.3
A35	–	–	–	–	1.6
A4	5.4	0.9	1.3	1.3	1.2
A45	–	–	–	–	1.4
A5	4.5	0.9	0.8	1.3	1.8
A7	–	0.3	2.5	6.3	4.0
A9	–	4.6	0.9	4.6	9.9
A11	–	–	0.9	2.4	9.5
A13	–	–	2.4	5.5	1.6
A15	–	–	4.1	10.2	5.5
A17	–	–	11.8	14.0	14.6
A19	–	–	11.4	10.1	13.4
A21	–	–	10.1	16.5	11.9

North

ST

South

2011

	Jan	Mar	May	Jul	Oct
A1	–	–	–	–	–
A2	2.4	1.6	1.7	2.1	3.7
A25	2.2	2.1	–	5.3	3.0
A3	3.9	1.8	1.5	4.2	3.1
A35	3.7	1.7	–	2.3	2.5
A4	4.1	2.8	1.4	6.5	2.5
A45	4.4	–	–	5.8	5.2
A5	2.8	4.2	3.1	2.2	8.6
A7	3.3	5.0	1.4	1.9	10.0
A9	3.3	2.1	1.9	7.5	9.6
A11	2.5	2.8	2.0	1.8	1.9
A13	–	1.9	1.6	6.0	5.8
A15	–	4.0	1.7	8.2	12.2
A17	–	4.7	7.8	10.3	10.8
A19	–	3.9	–	10.3	11.9
A21	–	11.0	–	6.4	11.8

2012

	Jan	Mar	May	Jul	Oct
A1	–	–	–	–	–
A2	2.1	0.2	1.5	7.1	5.4
A25	–	–	–	1.2	2.0
A3	1.6	0.8	4.1	3.4	2.0
A35	–	–	–	1.3	1.4
A4	3.9	1.0	0.9	1.2	1.4
A45	–	–	–	4.4	2.7
A5	3.7	0.8	0.9	1.2	4.1
A7	–	0.8	0.8	1.3	6.5
A9	4.9	1.4	5.3	3.2	–
A11	3.1	4.4	7.7	2.3	–
A13	6.3	5.1	7.6	2.5	–
A15	–	10.3	3.8	4.8	–
A17	10.5	9.4	9.3	10.2	10.0
A19	10.4	9.2	10.3	10.4	10.5
A21	11.5	10.0	10.0	–	10.5

2013

	Jan	Mar	May	Jul	Oct
A1	–	–	–	–	–
A2	1.1	0.8	0.2	7.1	3.1
A25	1.7	0.5	4.3	1.2	3.8
A3	1.3	2.8	3.3	3.4	3.1
A35	1.2	3.1	2.9	1.3	2.1
A4	1.9	3.0	5.8	1.2	2.5
A45	1.9	2.7	3.5	4.4	3.7
A5	1.7	–	1.7	1.2	3.5
A7	5.2	–	2.7	1.3	2.8
A9	3.1	–	6.9	3.2	14.1
A11	3.1	–	5.8	2.3	14.6
A13	3.6	–	7.0	2.5	1.6
A15	10.8	–	12.8	4.8	4.1
A17	9.3	–	11.2	9.3	1.7
A19	9.1	–	11.9	10.4	7.3
A21	9.8	–	13.2	11.4	16.8

2014

	Jan	Mar	May	Jul	Oct
A1	–	–	–	–	–
A2	1.8	0.2	0.4	4.4	5.7
A25	2.0	1.9	0.5	4.7	–
A3	2.2	2.3	1.0	3.7	4.7
A35	1.7	1.4	1.4	3.4	–
A4	2.0	3.9	1.4	2.3	4.2
A45	1.8	1.4	1.8	6.1	–
A5	2.1	2.0	1.9	4.4	3.5
A7	4.6	1.5	3.9	4.4	2.1
A9	3.3	6.1	4.4	10.6	1.9
A11	5.0	6.3	4.0	7.1	2.4
A13	5.2	5.1	4.7	2.3	1.9
A15	5.3	4.6	4.6	1.6	2.5
A17	2.5	6.9	8.3	6.5	3.2
A19	8.8	10.8	10.7	2.6	12.3
A21	14.2	10.8	9.1	15.9	11.9

2015

	Jan	Mar	May	Jul	Oct
A1	–	–	–	–	–
A2	3.0	0.9	2.9	7.5	8.1
A25	2.2	–	–	7.6	6.6
A3	2.5	1.6	–	5.4	5.6
A35	3.7	–	–	5.3	5.8
A4	3.5	1.0	1.6	5.1	10.3
A45	3.2	–	–	4.5	9.7
A5	2.4	1.8	3.9	5.0	9.0
A7	5.0	1.9	3.6	9.1	9.9
A9	4.5	7.6	7.4	9.1	9.4
A11	4.3	7.2	8.3	7.8	6.5
A13	5.0	7.5	6.7	9.4	5.8
A15	10.8	6.3	11.9	9.6	5.9
A17	12.3	9.4	11.4	12.9	7.2
A19	–	12.1	10.3	12.4	5.7
A21	–	–	10.4	10.7	10.1

2016

	Jan	Mar	May	Jul	Oct
A1	–	–	–	–	–
A2	2.4	0.5	7.7	4.8	7.1
A25	–	0.5	8.3	6.7	7.0
A3	5.5	0.5	8.5	8.9	6.7
A35	–	–	4.8	10.1	4.0
A4	1.9	0.8	0.9	10.5	3.9
A45	–	0.8	0.8	11.0	2.1
A5	1.9	0.8	0.8	10.6	1.5
A7	8.7	1.5	8.5	9.6	4.4
A9	10.2	9.1	9.1	10.6	1.8
A11	10.0	8.7	9.4	1.6	1.9
A13	9.5	3.3	8.1	1.1	2.6
A15	7.1	4.0	1.3	1.5	9.3
A17	8.9	14.0	6.7	9.7	15.8
A19	10.5	13.9	14.2	12.4	17.0
A21	15.1	11.9	13.6	13.2	16.8

2017

	Jan	Mar	May	Jul	Oct
A1	–	–	–	–	–
A2	2.7	0.6	1.0	2.2	–
A25	2.7	1.2	1.0	2.4	–
A3	3.2	1.8	1.2	1.7	–
A35	6.0	1.3	1.6	1.7	–
A4	3.6	1.4	1.4	1.6	–
A45	4.2	1.1	1.9	1.8	–
A5	3.3	1.7	1.8	1.7	–
A7	11.2	1.9	1.6	1.7	–
A9	4.7	2.9	7.2	8.6	–
A11	2.2	6.3	9.5	8.8	–
A13	3.4	2.2	8.2	2.2	–
A15	9.8	4.3	2.1	2.8	–
A17	10.2	8.1	10.0	8.2	–
A19	13.4	10.8	11.2	10.8	–
A21	15.9	11.1	11.3	12.2	–

[Figure R18-25] Salinity (a) and temperature (b) at 100m depth in each month and each station from 2007 to 2017.

7.2. Euphausiids

(Okazaki)

The community structure and distributional patterns of euphausiids along A-line coincided well with physical oceanographic features in the Oyashio region and the mixed water region (Sogawa et al. 2013). Forty species were detected in this area. The six dominant species were identified in cold-water: *Euphausia pacifica*, *Thysanoessa inspinata*, *Tessarabrachion oculatum*, *Thy. longipes*, *Thy. inermis* and *Thy. raschi*. On the other hand, the thirteen species dominating in the mixed water region were identified: *Nematoscelis difficilis*, *E. gibboides*, *E. similis*, *E. recurva*, *E. hemigibba*, *N. microps*, *Nematobrachion boopis*, *Bentheuphausia amblyops*, *Stylocheiron maximum*, *E. mutica*, *S. abbreviatum*, *Thysanopoda orientalis* and *N. atlantica*. Regarding the vertical distribution of four dominant species in the Oyashio region (Sogawa et al. 2016), *E. pacifica* is a surface migrant and *Tess. oculatum* is a moderate subsurface migrant. *Thy. inspinata* and *Thy. longipes* segregated vertically between *E. pacifica* and *Tess. oculatum* at night. Therefore, only *E. pacifica* are able to live in warmer temperatures and higher chlorophyll *a* in the surface layer. The reason why *E. pacifica* is the dominant species in the area is that they can undergo a food rich environment at the surface layer by adapting the warmer temperature. Taki (2012) also suggested that difference of the temperature tolerances may strongly affect the distributional pattern and the dominance of euphausiids off northeastern Japan.

Euphausiid samplings (bongo net tow from ca. 500 m depth to surface) at five stations along A-line have continued since 2006. The mean euphausiid biomass obtained in July changed annually (Figure R18-26). Negative anomalies of the biomass were detected in 2008, 2010 and the years after 2013. Further, the euphausiid biomass was correlated negatively with 200-m depth temperature (r = −0.56). Because the community structure and distributional patterns of euphausiids corresponded to water mass structures as mentioned above, annual changes of local oceanographic features such as temperature is likely to affect the euphausiid biomass and composition in the western North Pacific.

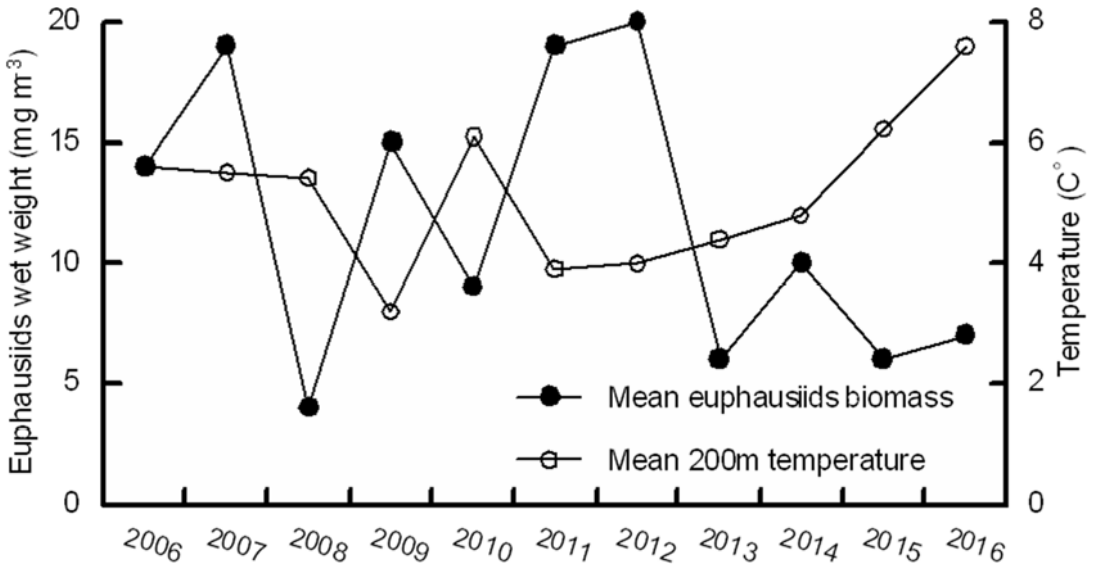

[Figure R18-26] Annual changes of mean euphausiids biomass and 200-m depth temperature in July at five stations (Stns. A04, A09, A13, A17 and A21) along A-line during 2006 to 2016.

8. Fish

8.1. Pelagic fish and squid

(Furuichi, Yukami, Kamimura, Kaga, Kidokoro)

Japanese fishers have been harvesting various marine organisms in the Oyashio, Kuroshio and its adjacent regions for a very long time. Small pelagic fish such as Japanese sardine (*Sardinops melanostictus*), Japanese anchovy (*Engraulis japonicus*), chub mackerel (*Scomber japonicus*), Pacific saury (*Cololabis saira*) and Japanese flying squid (*Todarodes pacificus*) have constituted most of the commercial landings since the early 20th century, but the landings have varied considerably (Figure R18-27). These species undergo seasonal north-south migrations between spawning grounds in the subtropical, Kuroshio region (see Sugisaki et al. 2010) during autumn-winter-spring and feeding grounds in the subarctic Oyashio water in summer. One of the distinctive features of the Kuroshio-Oyashio system is the large latitudinal contrast of environments. The dominant zooplankton size increases with latitude, and the start of active plankton production is earlier in the year in the south than in the north. Therefore, ontogenetic migration in the Kuroshio-Oyashio system favors small pelagic fish (Ito et al. 2004). Consistent with this "surf riding theory", reproduction occurs on time and space scales that take advantage of the “wave” of food supply that propagates from south to north (Pope et al. 1994). The spawning grounds of these species usually extend from Kyushu Island (southern Japan) to Cape Inubo (36ºN), except for the flying squid, which has its major spawning grounds in the East China Sea in winter, and for anchovy and Pacific saury, whose spawning grounds extend from southern Japan to the extensive area of the Transition Zone, presumably beyond the International Date Line in recent years when stock level has been high (anchovy) or to the California Current (Pacific saury). Biomass patterns and Japanese commercial catches of these small pelagic fishes indicate decadal changes or alternations of dominant species called “species replacements” (Figures R18-27 and 28). Although mechanisms of species replacements have not been fully resolved, ocean-climate regime shifts together with species interactions have profound impacts on dynamics of small pelagic fishes.

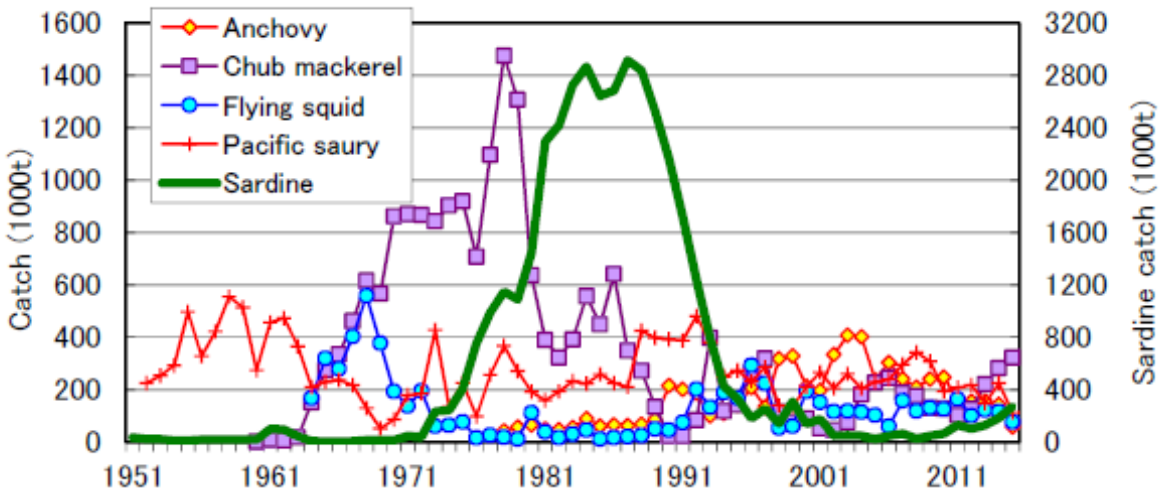

[Figure R18-27] Japanese catch of sardine, anchovy, chub mackerel, Pacific saury and flying squid (winter spawning stock) along the Pacific coast of Japan. Japanese flying squid catches include the catches in the Okhotsk Sea and the Nemuro Strait.

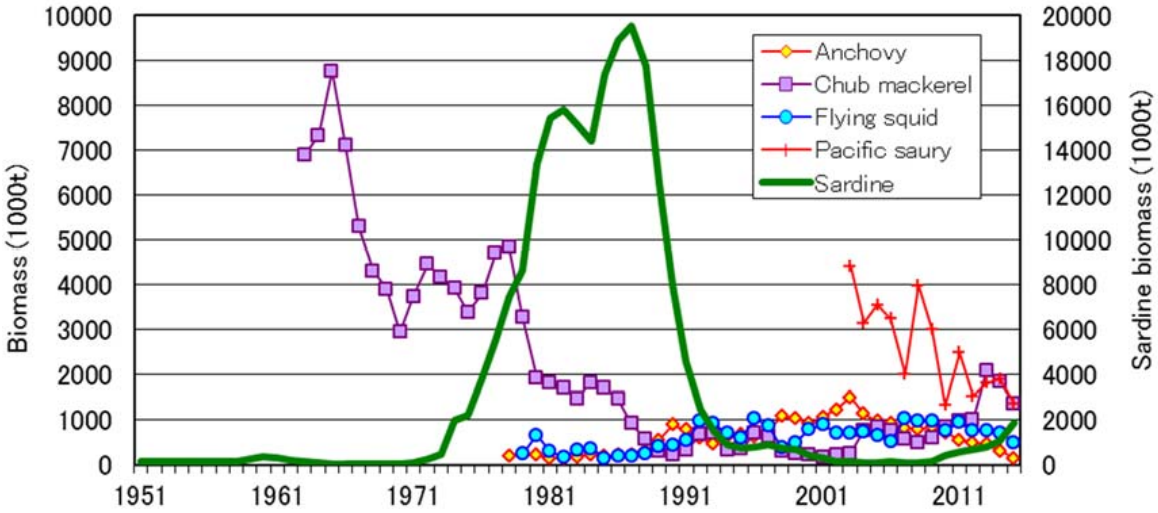

[Figure R18-28] Biomass of sardine, anchovy, chub mackerel, Pacific saury and flying squid (winter spawning stock) along the Pacific coast of Japan. NB: anchovy biomass represents only Japanese coastal and offshore waters. Biomass of Pacific saury was estimated for western and central North Pacific west of 177ºW

Sardine biomass and catch were high during the 1980s and decreased in the 1990s. The onset of increase and decrease of the biomass occurred in the early 1970s and 1989, respectively, which coincided with regime shifts found in sea surface temperature (SST) and mixed layer depth (Nishikawa and Yasuda 2008) around the Kuroshio Extension.

Reproductive success, which is determined by interannual changes in survival rates of larvae and juveniles, is affected by the SST of the Kuroshio Extension southern area and locations around the southern boundary of the Oyashio intrusion. Spawning stock biomass (SSB) was around 0.5 million t in the late 1990s and has decreased to less than 0.1 million t since 2002. Therefore, recruitment and catch have been extremely low in the 2000s. However, good recruitment has occurred since 2010, and SSB and catch have been increasing in recent years. Mean body weight of age 0–2 sardines was low during the 1980s when sardine biomass was high. It suddenly increased in the early 1990s, and then, no obvious change has been observed (Figure R18-29).

Chub mackerel biomass and catch were high during the 1970s and decreased in the early 1990s, thereafter increasing slightly. Despite the occurrences of strong year-classes in 1992 and 1996, intensive fishing on immature fishes prevented stock recovery. In 2004, an occurrence of a strong year-class together with a “stock recovery plan” slightly improved stock biomass and catch in subsequent years. Thus, recruitment and catch since the 1990s have been variable. The biomass of chub mackerel fluctuated between 0.15 million t (2001) and 2.07 million t (2013) after 2000. The mean body weight of age 0–2 chub mackerel was low until the mid-1980s, when chub mackerel biomass was high, and gradually increased in the late 1980s (Figure R18-29).

Anchovy and flying squid biomass and catch have been relatively high since the 1990s, but with considerable year-to-year fluctuations (e.g. a drastic decline of squid catch in 1998 and 1999 when an extremely strong El Niño occurred), which reflected their relatively short life spans (2 or 3 years for anchovy and 1 year for squid). The biomass of anchovy decreased gradually from 2003 (1.5 million t) to 2015 (0.2 million t). The biomass of flying squid fluctuated between 0.7 and 1.0 million t between 2009 and 2014 and decreased to 0.5 million t in 2015. The biomass in 2015 was lower compared to biomass trends since 1990s. Low reproductive success in 2015 could be attributed to low winter SST in the main spawning grounds (East China Sea).

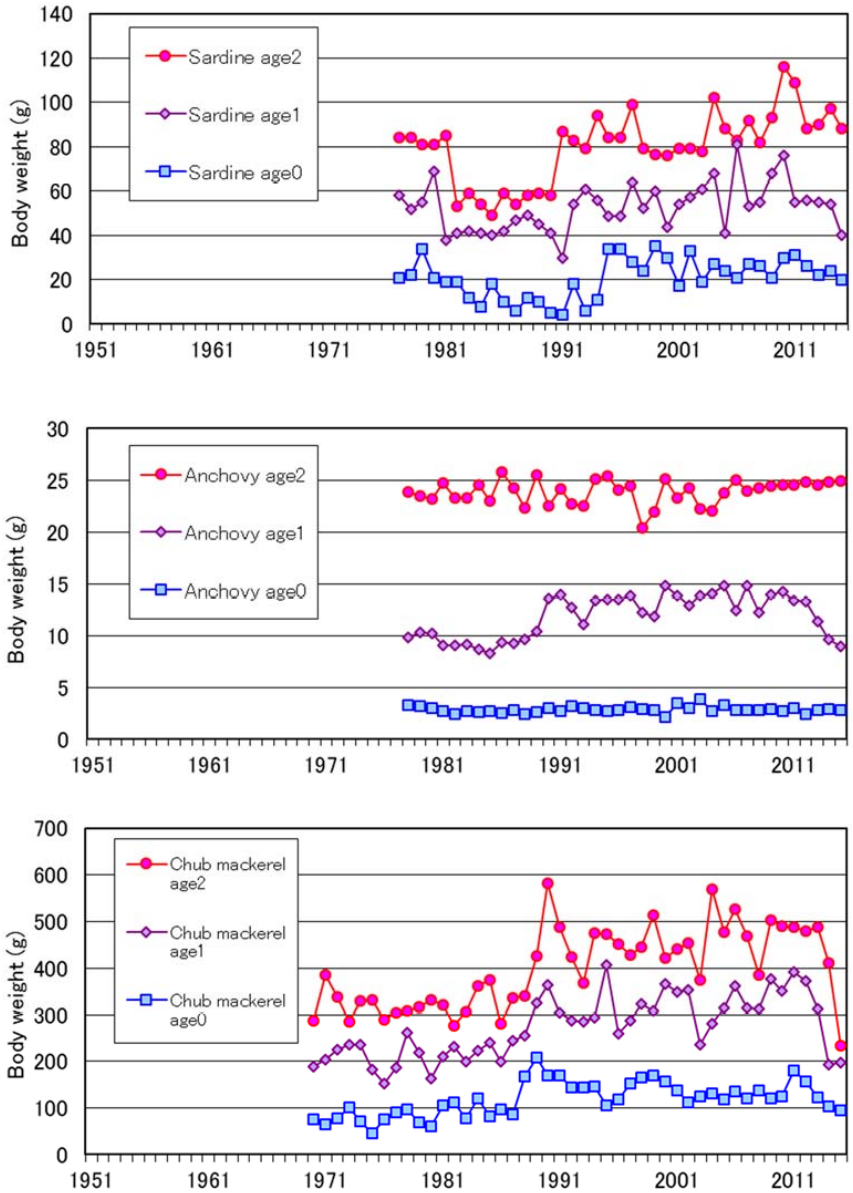

[Figure R18-29] Mean body weight by age of sardine, anchovy and chub mackerel along the Pacific coast of Japan

The catch and biomass of sardine seem to be negatively related with those of anchovy and flying squid. The mean body weight of age 0–2 anchovy has been relatively stable since the late 1970s, except for a slight increase in body weight of age-1 fish in the late 1980s, which coincided with the increase in body weight of chub mackerel (Figure R18-29).

The catch of Pacific saury by Japanese fisheries fluctuated in the range of 0.2–0.35 million t during 1990s and 2000s except in 1998 and 1999 in which the stock size of Pacific saury declined abruptly. Saury catch tended to decrease after 2010, although the catches by Chinese Taipei's and Chinese fisheries tended to increase. It is considered that the decline of the catch of the Pacific saury by Japanese fisheries after 2010 was caused by the decline of stock size and immigrants into the water around the Japanese Islands which was observed by the Japanese fisheries-independent surveys.

8.2. Pacific salmon

(Saito)

Six species of Pacific salmon [chum salmon (*Oncorhynchus keta*), pink salmon (*O. gorbusha*), masu salmon (*O. masou*), sockeye salmon (*O. nerka*), coho salmon (*O. kisutch*), Chinook salmon (*O. tschawytscha*)], and steelhead trout (*O. mykiss*) are harvested in the coastal waters along the Pacific coast of Hokkaido and Honshu. Of these salmonids, the first three species are abundant, and consequently the most important targets for the Japanese salmon fishery. The annual catch of each of the other four species was ca. 0–80 metric tonnes in the coastal waters of all of Japan during the last 10 years (2007–2016), except the coho catch in 2011, which was about 1,400 metric tonnes. The high catch of coho salmon in 2011 was due to escapees from pen-culture facilities in the Sanriku region, the northeastern Pacific coastal area of Honshu, where the Great East Japan Earthquake struck on March 11, 2011.

Spawning populations of chum, pink, and masu salmon exist in northern Japan, although those of pink salmon occur mainly on the Okhotsk coast of Hokkaido. A few sockeye salmon occasionally return from the ocean as adults to Lake Kusshar o (43°38'N 144°20'E) in the Kushiro River system, Hokkaido, which is derived from a lacustrine conspecific population (Kasugai et al. 2014). These four species are also artificially propagated in hatcheries: the annual numbers of chum and pink salmon released from Japan have been kept almost constant since the 1980s and 1990s, respectively (chum: 1.6–2.1 billion, pink: 102–151 million). The numbers of released masu salmon have ranged from 7.7 million to 17.4 million since the early 1990s, and those of sockeye salmon have decreased gradually from 2.9 million in 1992 to ca. 0.2 million in 2013–2015 (NPAFC 2017). The contribution of hatchery fish to total commercial catches is estimated to be 70% for chum salmon, and 20–30% for pink and masu salmon (Morita 2014). Although the contribution of hatchery-origin sockeye salmon to coastal catch is unknown, several tens to hundreds of adult sockeye salmon return to their rivers of release (e.g., the Abira, Shizunai, and Kushiro Rivers) every year. Sockeye, coho, Chinook salmon, and steelhead trout, as well as some chum and pink salmon caught during spring and early summer in the coastal waters of northern Japan, are thought to be fish in their feeding or spawning migrations.

The chum salmon catch in Japan has increased since the mid-1970s. It reached the highest level of 266 thousand metric tonnes in 1996, decreased to 140 thousand metric tonnes in 2000, and recovered to 257 thousand metric tonnes in 2003 (Figure R18-30a). However, catch has decreased gradually since then and reached 95 thousand metric tonnes in 2016, which was the lowest level in the last 34 years. The chum salmon catch on the Hokkaido Pacific side showed a similar annual pattern to total catch. The catch on the Honshu Pacific side decreased abruptly in 1999, and the 1999 level was maintained until 2009. However, chum salmon catches have decreased further since 2010 on both the Hokkaido and Honshu Pacific sides. The reasons for these recent declines are unknown, but a recent study demonstrated that a decrease in return rates for chum salmon to Iwate Prefecture, the most productive area for chum salmon on the Honshu Pacific coast, is linked to an increased frequency of juveniles residing in the warm coastal water (Wagawa et al. 2016). Although it might be difficult to understand the decreased chum salmon catch on the Hokkaido Pacific side with the same explanation shown by Wagawa et al. (2016), their findings provide valuable insight to resolve the recent declines in chum salmon along the Pacific coast of Japan. Another possible reason for the decreased chum salmon catch could be increased predation on chum salmon juveniles during their coastal residency by predatory fish, such as masu salmon and walleye pollock (*Theragra chalcogramma*). For example, masu salmon have been identified as an important predator of chum juveniles even at the smolt life stage, as well as immature fish (Nagasawa and Mayama 1997). The average annual catch of masu salmon in Pacific coastal waters of Hokkaido was 0.37 thousand metric tonnes during 1992–2006, but the annual catch increased abruptly to 0.47–0.82 thousand metric tonnes during 2007–2011 (Figure R18-30c). In fact, a three-year lagged time-series of chum catch (t-3: t = 1995–2016) on the Hokkaido Pacific side was significantly correlated with the time

series of masu salmon catch (t': t'=1992–2013) in the same area ($r = -0.51$, $p < 0.05$), suggesting the possibility that immature masu salmon fed on out-migrating chum juveniles in coastal waters when the return age of chum salmon is assumed to be 4 years old, which is the dominant age at return for Japanese chum salmon. As chum salmon juveniles originating from the Honshu Pacific side also migrate along the Hokkaido Pacific coast toward the Sea of Okhotsk (Irie 1990), the same predation impact of masu salmon is supposed.

The catch of pink salmon in Japan was predominantly in even-numbered years compared with odd-numbered years during the 1990s and early 2000s (Figure R18-30b). However, the dominance was reversed in 2003–2004: the 2003 catch (18.5 thousand metric tonnes) was very close to that in 2002 (19.6 thousand metric tonnes) but the 2004 catch (9.2 thousand metric tonnes) fell to almost half of the 2003 catch. Since then, the odd-numbered years have become predominant. The pink salmon catch decreased for both odd- and even- numbered year lines during 2011–2015 in Japan, but the 2016 catch reached the highest level among the even-numbered years after 2004. The reasons for the declines during 2011–2015 were proposed to be due to low sea surface temperatures (SSTs) during coastal residency of juveniles and higher SSTs during spawning migrations of adult fish and/or loss of diversity of spawning timing caused by artificial selection for early spawning fish in hatcheries during the mid-1980s and mid-1990s (Saito et al. 2016). The catches on the Hokkaido Pacific side contained mostly adult pink salmon heading to their natal rivers on the Okhotsk coast of Hokkaido, which are caught in coastal fisheries during August and September, but those in the Honshu Pacific side are fish undertaking an oceanic feeding migration during spring and early summer. Catches on the Honshu Pacific side have dropped to lower levels since 1999, suggesting that the oceanic distribution of pink salmon has changed compared with that in previous years.

The catch of masu salmon ranged from 0.7 thousand to 2.2 thousand metric tonnes during 1992–2016 in Japan (Figure R18-30c). Annual variability in catch seemed to be larger on the Hokkaido Pacific side [coefficient of variation (CV) = 0.38] than on the Honshu Pacific side (CV = 0.27). As mentioned above, the annual catch on the Hokkaido Pacific side increased abruptly during 2007–2011 and was maintained or exceeded a similar level of the average annual catch of 1992–2006 after 2012. The reasons for the increased masu salmon catch on the Hokkaido Pacific side are unknown, but Morita (2014) hypothesized climatic changes, because Russian catches of coho salmon, a species with a life history similar to that of masu salmon, appeared to be synchronized with the masu catches in Hokkaido.

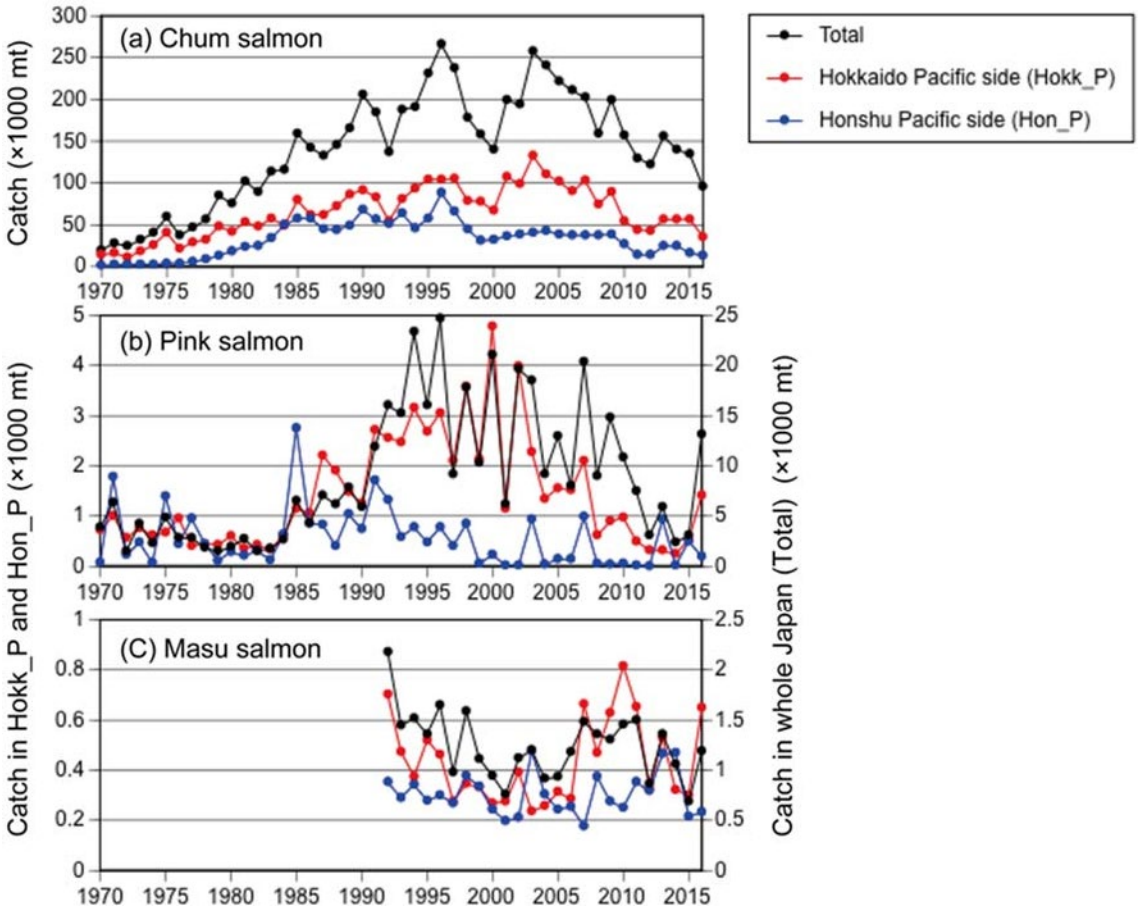

[Figure R18-30] Commercial catches of (a) chum, (b) pink, and (c) masu salmon on the Hokkaido Pacific side (red lines), the Honshu Pacific side (blue lines), and all of Japan (black lines). The data sources refer to the NPAFC Statistics (http://www.npafc.org/new/science_statistics.html). As regional catches of all species were unknown in the original 2006–2014 dataset, the regional catches of each species were calculated from the regional proportions of catches shown in the NPAFC Docs. 1048, 1140 (Rev.1), 1344, 1401, 1465, 1515, and 1585. Regional catches for 2008 and 2009 were estimated from unpublished data collected by the former Hokkaido National Fisheries Research Institute, and Japan Fisheries Research and Education Agency, Sapporo, Japan (currently, Salmon Research Department, Fisheries Resources Institute, Sapporo, Japan), due to the lack of information available on regional catches in NPAFC Docs. 1183 and 1259

9 Sea bird and marine mammal

9.1. Status of breeding seabirds along Pacific coast of Hokkaido

(Watanuki)

On the islands along the Pacific coast of eastern Hokkaido, 9 species of seabirds have been recorded to breed. Information on the status of Leach's Storm-Petrels (*Oceanodroma lencorhoa)* and Ancient Murrelets (*Synthliboramphus antiquus*) are limited. The interannual change of populations of other 7 species since 1960s to 2013 will be described basing on the Seabird's Colony Database and data from MONITORING 1000 program by Ministry of the Environment Japan (https://www.sizenken.biodic.go.jp/seabirds/).

Black-tailed Gulls were recorded to breed on Daikoku, Yururi and Moyururi Islands. The number of adults counted in breeding sites during the spring and summer were less than 100 before 2000 but can be more than 1000 afterwards (Figure R18-31). Contrarily, the numbers of adults of Slaty-backed gulls (*L. schstisagus* that breed mainly on Daikoku, Yururi and Moyururi Islands observed in the breeding sites increased until 1980s and peaked (20,000 birds in total) around the 1980s and 1990s then decreased afterwards (Figure R18-31). The number of nests of Japanese Cormorants (*Pharacrocorax filamentosus*) on Moyururi, Yururi and Daikoku Islands varied between 100 and 300 and showed no apparent interannual trends, while the number of Red-faced Cormorants (*P. urile*), that breed on Yururi and Moyururi Islands declined between 1960 and 1980, continuing at lower than 20 nests (Figure R18-31).

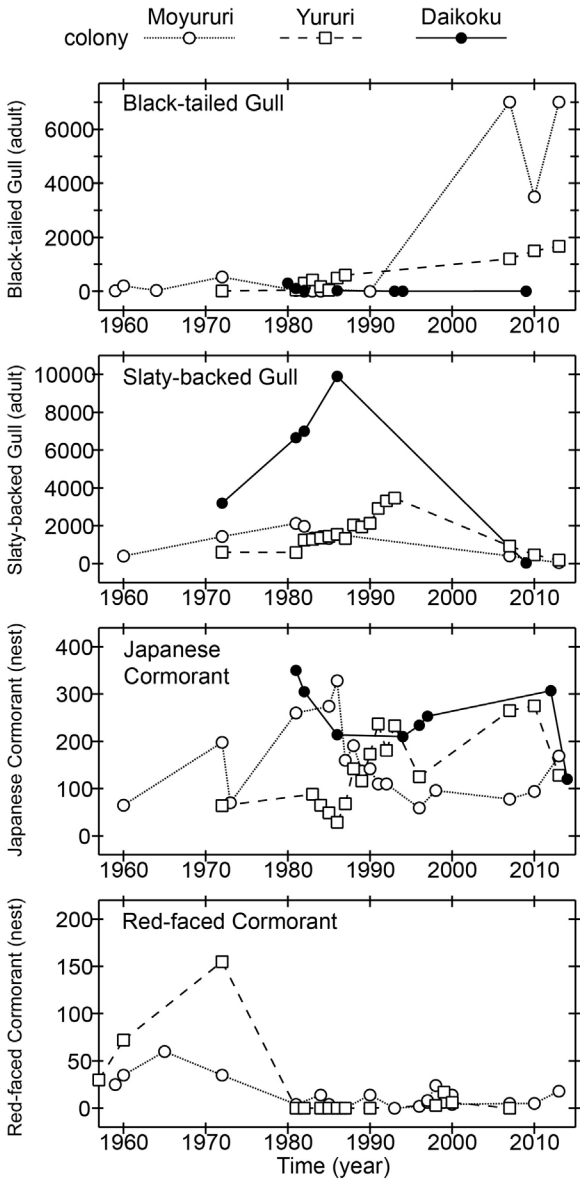

[Figure R18-31] Trends of the number of adults or number of nests of gulls and cormorants breeding in eastern coast of Hokkaido.

Four species of alcids showed contrasting population trends in 1960s and 2010s along the Pacific coast of eastern Hokkaido (Figure R18-32). Common Murres (*Uria aalge*) were reported to breed on Moyururi Island before 1970's but its numbers on breeding sites declined since then and breeding was not observed afterwards. Tufted Puffins (*Fratercula cirhata*), that breed on Yururi and Moyururi Islands, showed a similar trend; they declined from the 1970's to the 1990s and did not show recovery. The number of adults of Spectacled Guillemots (*Cepphus carbo*) observed on the water near potential breeding sites along the cliffs declined both at Moyururi and Yururi Islands between the 1970s and the 1990s but seemed to slightly increase in 2000s. Contrarily, population of Rhinoceros Auklets appeared to increase slightly in 1960s to 201's.

The factors affecting these changes seabird's populations are unclear. Foxes, Norwegian rats, and white-tailed sea eagles were recognized as potential threats on Daikoku, Yururi and Moyururi Islands. Disturbance of breeding birds by white-tailed sea eagles is often observed at Daikoku Island. By-catch by coastal gillnets might be a concern. In addition to these local anthropogenic and predator impacts, the meso-scale climate change and the concordant

changes of fish stocks might influence the change of seabird populations in northern Japan. Japanese anchovy is the preferred prey species for increased growth and survival of the chicks of Rhinoceros Auklets. Thus the population increase of this species in 1990s and 2000s, that was also observed at two colonies off west coast Japan (NPRES Regions 19), might be attributed to the high availability of anchovy. The populations of Spectacled Guillemots on the islands of the same region showed similar trend; declined until 1990s then increased afterwards, indicating an influence of meso-scale ecosystem change in northern Japan.

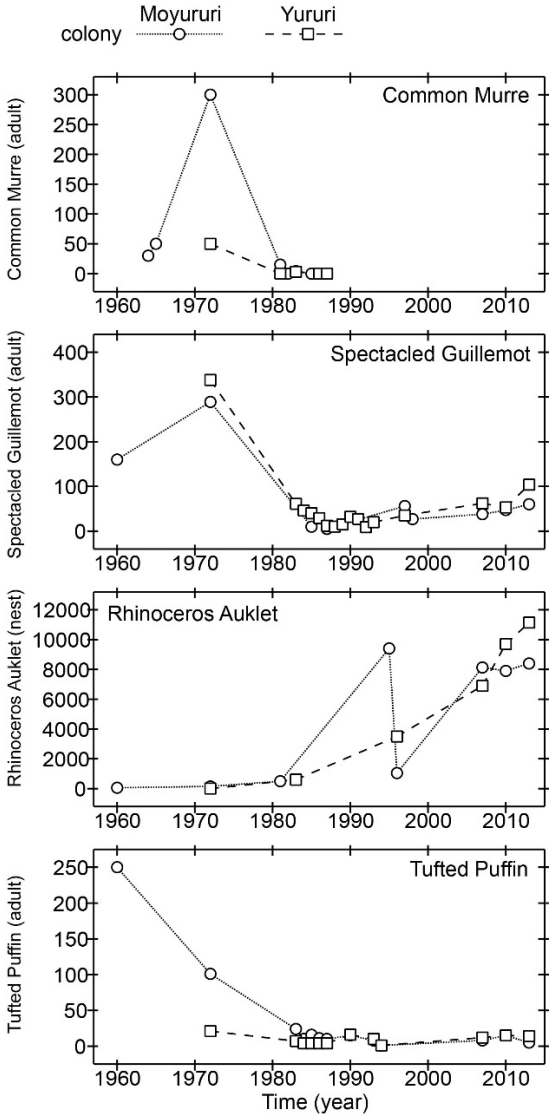

[Figure R18-32] Trends of the number of adults or number of nests of four species of alcids breeding in eastern coast of Hokkaido.

9.2. Pinnipeds

(Yamamura)

Steller sea lions (SSLs) distributed in the Kuril Island comprise the Asian stock along with those from Okhotsk and Kamchatka. However, the stock has fluctuated with contrasting trends among natal areas; whereas those in Kamchatka are still stagnating after the steep decline by the beginning of 1990s, SSLs from Okhotsk and Kuril have increased at a relatively steady rate of 4 % yr^{-1} by 2012, based on the monitoring continued by Russian and Japanese scientists. This recovery also seriously impacted Japanese coastal fishery, especially in the west coast of Hokkaido Island, by breaking fishing nets and depredations. SSLs have been culled in this area, but the number culled has been rather moderate between 1993–2014. In 2012, SSL was downlisted from “Endangered” to “Near Threatened” in both red lists of IUCN and Japan Ministry of Environment, and then Japan started population control of SSL in western Hokkaido in the period of 2014–2023. To accomplish the control, Japan is now culling ca. 500 SSLs a year. This increased culling pressure appears to have affected the hauling out behavior of SSLs in the past two seasons, but the effect on the population dynamics remains still unclear.

However, in 2016, decreased pup production was observed in Kuril Islands after 20 years of an increasing trend, while SSLs in Sakhalin and northern Okhotsk continued to increase (Muto et al., 2021). The decline of pup production which occurred only in the Kuril Archipelago may be related to the bottom-up forcing in the positive (cold) phase of PDO in the western NPO. In May 2016, an unprecedented superabundance of SSLs (>5,000) was observed on and near Benten Rock, near Cape Soya situated on the northern tip of Hokkaido Island (Figure R18-33). Usually SSLs are low in number in May, since they migrate to Russian waters to reproduce. Although there was no plausible explanation for the superabundance of SSLs, they may have aggregated for certain prey (e.g. sand lance -*Ammodytes* spp.).

The Kuril harbor seal *Phoca vitulina tejnegeri* and the spotted seal *Phoca largha* are commonly found along the Hokkaido coast. Although spotted seals used to be seasonal migrators that were distributed here only during winter, some fraction of the seals persist throughout the year in some sites of Hokkaido (e.g. Yagisihi and Rebun Islands, along the west coast) in recent years, and the hauling out sites are extending south. Kuril harbor seal is the only species that reproduce on the shores of Hokkaido. This species once declined to near-extinction level in Hokkaido waters, but recovered by 2010 (Kobayashi et al., 2015). Since both species are causing fishing damage especially with the salmon set net fishery, approximately 100 seals per year are culled.

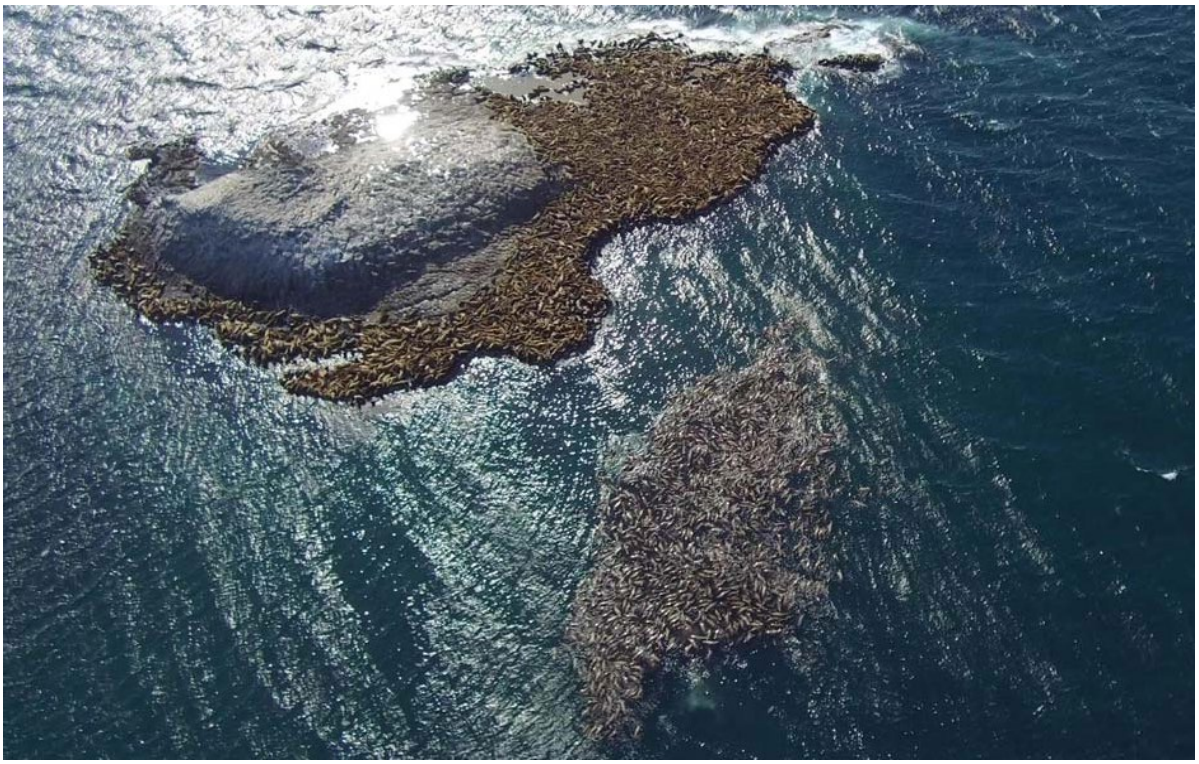

[Figure R18-33] Superabundance of Steller sea lions on and near the Benten Rock in the Soya Strait, northern tip of the Hokkaido Island in May 2017. This photo was taken using an UAV. (Photo courtesy of Yoko Goto, Wakkanai Fisheries Research Institute)

Acknowledgements

The leading author would like to deeply thank M. Nakagami, from the Japan Fisheries Research and Education Agency for dedicated support to summarize the Pelagic fish and squid section (Section 8.1).

10 References

Aakrog, A. 2003. Input of anthropogenic radionuclides into the world ocean. Deep-Sea Research Part-II 50: 2597–2606. https://doi.org/10.1016/S0967-0645(03)00137-1

Andreev, A.G., Kusakabe, M. 2001. Interdecadal variability in dissolved oxygen in the intermediate water layer of the Western Subarctic Gyre and Kuril Basin (Okhotsk Sea). Geophysical Research Letters 28: 2453–2456. https://doi.org/1 0.1029/2000GL012688

Aoyama, M., Uematsu, M., Tsumune, D., Hamajima, Y. 2013. Surface pathway of radioactive plume of TEPCO Fukushima NPP1 released ^{134}Cs and ^{137}Cs. Biogeosciences 10: 3067–3078. https://doi.org/10.5194/bg-10-3067-2013

Aoyama, M. Hamajima, Y., Hult, M., Uematsu, M., Oka, E., Tsumune, D., Kumamoto, Y. 2016. ^{134}Cs and ^{137}Cs in the North Pacific Ocean derived from the TEPCO Fukushima Dai-ichi Nuclear Power Plant accident, Japan in March 2011: Part One –Surface pathway and vertical distributions. Journal of Oceanography 72: 53–65. https://doi.org/10.1007/s10872-015-0335-z

Bowen, V.T., Noshkin, V.E., Livingston, H.D. and Volchok, H.K. 1980. Fallout radionuclides in the Pacific Ocean: Vertical and horizontal distributions, largely from GEOSECS stations. Earth and Planetary Science Letters 49: 411–434. https://doi.org/10.1016/0012-821X(80)90083-7

Buesseler, K.O., Aoyama, M. and Fukasawa, M. 2011. Impacts of the Fukushima Nuclear Power Plants on marine radioactivity. Environmental Science and Technology 45: 9931–9935. https://doi.org/10.1021/es202816c

Burkanov, V.N., Artemeva, S. M., Hattori, K., Isono, T., Permyakov, P. A., Tretyakov, A. V., 2015. Results of a brief survey of Steller sea lions (*Eumetopias jubatus*) in the northern Sea of Okhotsk and the coast of Sakhalin Island, 2013. Proceedings of Eighth International Conference on Marine Mammals of the Holarctic, pp. 108–112.

Chiba, S., Tadokoro, K., Sugisaki, H. and Saino, T. 2006. Effects of decadal climate change on zooplankton over the last 50 years in the western subarctic North Pacific. Global Change Biology 12: 907–920. https://doi.org/10.1111/j.1365-2486.2006.01136.x

Chiba, S., Aita, M.N., Tadokoro, K., Saino, T., Sugisaki, H. and Nakata, K. 2008. From climate regime shifts to lower-trophic level phenology: Synthesis of recent progress in retrospective studies of the western North Pacific. Progress in Oceanography 77: 112–126. https://doi.org/10.1016/j.pocean.2008.03.004

Chiba S., Sugisaki, H., Nonaka, M. and Saino, T. 2009. Geographical shift of zooplankton communities and decadal dynamics of the Kuroshio–Oyashio currents in the western North Pacific. Global Change Biology 15: 1846–1858. https://doi.org/10.1111/j.1365-2486.2009.01890.x

Chino, M., Nakayama, H., Nagai, H., Terada, H., Katata, G., Yamazawa, H. 2011. Preliminary estimation of release amounts of ^{131}I and ^{137}Cs accidentally discharged from the Fukushima Daiichi Nuclear Power Plant into the atmosphere. Journal of Nuclear Science and Technology 48: 1129–1134. https://doi.org/10.1080/18811248.2011.9711799

Gruber, N. 2011. Warming up, turning sour, losing breath: Ocean biogeochemistry under global change. Philosophical Transactions of the Royal Society A 369: 1980–1996. https://doi.org/10.1098/rsta.2011.0003

Hanawa, K., Mitsudera, H. 1987. Variation of water system distribution in the Sanriku coastal area. Journal of Oceanographical Society of Japan 42: 435–446. https://doi.org/10.1007/BF02110194

Hayakawa, M., Suzuki, K., Saito, H., Takahashi, K., Ito, S. 2008. Differences in cell viabilities of phytoplankton between spring and late summer in the northwest Pacific Ocean. Journal of Experimental Marine Biology and Ecology 360: 63–70. https://doi.org/10.1016/j.jembe.2008.03.008

Hirose, K., Aoyama, M. 2003. Present background levels of surface ^{137}Cs and ^{239,240}Pu concentrations in the Pacific. Journal of Environmental Radioactivity 69: 53–60. https://doi.org/10.1016/S0265-931X(03)00086-9

Honda, M.C., Aono, T., Aoyama, M., Hamajima, Y., Kawakami, H., Kitamura, M., Masumoto, Y., Miyazawa, Y., Takigawa, M., Saino, T. 2012. Dispersion of artificial caesium-134 and -137 in the western North Pacific one month after the Fukushima accident. Geochemical Journal 46: e1–e9. https://doi.org/10.2343/geochemj.1.0152

Hong, G.H., Baskaran, M., Povinec, P.P. 2004. Artificial radionuclides in the western North Pacific: A review. In Global Environmental Change in the Ocean and on Land. M. Shiyomi et al. (eds) Terapub, pp.147–172.

Huang, B., Banzon, V.F., Freeman, E., Lawrimore, J., Liu, W., Peterson, T.C., Smith, T.M., Thorne, P.W., Woodruff, S.D., Zhang, H.M. 2014. Extended reconstructed sea surface temperature version 4 (ERSST.v4): Part I. Upgrades and intercomparisons. Journal of Climate 28: 911–930. https://doi.org/10.1175/JCLI-D-14-00006.1

Irie, T. 1990. Ecological studies on the migration of juvenile chum salmon, *Oncorhynchus keta*, during early ocean life. Bullutine of Seikai National Fisheries Research Institute 68: 1–142 (In Japanese with English abstract).

Isoguchi, O., Kawamura, H., Oka, E. 2006. Quasi-stationary jets transporting surface warm waters across the transition zone between the subtropical and the subarctic gyres in the North Pacific. Journal of Geophysical Research 111: C10003. https://doi.org/10.1029/2005JC003402

Ito, S., Sugisaki, H., Tsuda, A., Yamamura, O., Okuda, K., 2004. Contributions of the VENFISH program: meso-zooplankton, Pacific saury (*Cololabis saira*) and walleye pollock (*Theragra chalcogramma*) in the northwestern Pacific. Fisheries Oceanography 13 (s1):1–9. https://doi.org/10.1111/j.1365-2419.2004.00309.x

Jo, H.-S., Yeh, S.-W., Kim, C.-H. 2013. A possible mechanism for the North Pacific regime shift in winter of 1998/1999. Geophysical Research Letters 40: 4380–4385. https://doi.org/10.1002/grl.50798

Kaeriyama, H., Ambe, D., Shimizu, Y., Fujimoto, K., Ono, T., Yonezaki, S., Kato, Y., Matsunaga, H., Minami, H., Nakatsuka, S., Watanabe, T. 2013. Direct observation of ^{134}Cs and ^{137}Cs in surface seawater in the western and central North Pacific after the Fukushima Dai-ichi nuclear power plant accident. Biogeosciences 10: 4287–4295. https://doi.org/10.5194/bgd-10-1993-2013

Kaeriyama, H., Shimizu, Y., Ambe, D., Masujima, M., Shigenobu, Y., Fujimoto, K., Ono, T., Nishiuchi, K., Taneda, T., Kurogi, H., Setou, T., Sugisaki, H., Ichikawa, T., Hidaka, K., Hiroe, Y., Kusaka, A., Kodama, T., Kuriyama, M., Morita, H., Nakata, K., Morinaga, K., Morita, T., Watanabe, T. 2014. Southwest intrusion of ^{134}Cs and ^{137}Cs derived from the Fukushima Dai-ichi Nuclear Power Plant accident in the western North Pacific. Environmental Science and Technology 45: 3120–3127. https://doi.org/10.1021/es403686v

Kaeriyama, H. 2015. Chapter 2. ^{134}Cs and ^{137}Cs in the seawater around Japan and in the North Pacific. In: Impacts of the Fukushima Nuclear Accident on Fish and Fishing Grounds. Nakata, K. and Sugisaki, H. (eds) Springer Japan, pp. 11–32.

Kaeriyama, H., Shimizu, Y., Setou, T., Kumamoto, Y., Okazaki, M., Ambe, D., Ono, T. 2016. Intrusion of Fukushima-derived radiocaesium into subsurface water due to formation of mode waters in the North Pacific. Scientific Reports 6: https://doi.org/10.1038/srep22010

Kaeriyama, H. 2017. Oceanic dispersion of Fukushima-derive radioactive cesium: a review. Fisheries Oceanography 26: 99–113. https://doi.org/10.1111/fog.12177

Kalnay, E., et al. 1996. The NCEP/NCAR 40-year reanalysis project. Bulletin of the American Meteorological Society 77: 437–471. https://doi.org/10.1175/1520-0477(1996)077<0437:TNYRP>2.0.CO;2

Kasai, H., Ono, T. 2007. Has the 1998 regime shift also occurred in the oceanographic conditions and lower trophic ecosystem of the Oyashio region? Journal of Oceanography 63: 661–669. https://doi.org/10.1007/s10872-007-0058-x

Kasugai, K., Hayano, H., Mano, S., Watanabe, T., Yoshikawa, T., Saito, M., Wakimoto, R. 2014. Upstream and downstream migration history of lacustrine sockeye salmon captured in Lake Kussharo estimated from otolith microchemistory (Short Paper). Science reports of Hokkaido Fisheries Research Institutes 86: 145–149 (In Japanese with English abstract).

Keeling, R.F., Körtzinger, A., Gruber, N. 2010. Ocean deoxygenation in a warming world. Annual Review of Marine Science 2: 199–229. https://doi.org/10.1146/annurev.marine.010908.163855

Kida, S., et al. 2015. Oceanic fronts and jets around Japan: a review. Journal of Oceanography 71: 469–497. https://doi.org/10.1007/s10872-015-0283-7

Kobayashi, T., Nagai, H., Chino, M., Kawamura, H. 2013. Source term estimation of atmospheric release due to the Fukushima Dai-ichi Nuclear Power Plant accident by atmospheric and oceanic dispersion simulations. Journal of Nuclear Science and Technology 50: 255–264. https://doi.org/10.1080/00223131.2013.772449

Kobayashi, Y., Kariya, T., Chishima, J., Fujii, K., Wada, K., Baba, S., Itoo, T., Nakaoka, T., Kawashima, M., Saito, S., Aoki, N., Hayama, S., Osa, Y., Osada, H., Niizuma, A., Suzuki, M., Uekane, Y., Hayashi, K., Kobayashi, M., Ohtaishi, N., Sakurai, Y. 2014. Population trends of the Kuril harbour seal *Phoca vitulina stejnegeri* from 1974 to 2010 in south eastern Hokkaido, Japan. Endangered Species Research 24: 61–72. https://doi.org/10.3354/esr00553

Kumamoto, Y., Aoyama, M., Hamajima, Y., Aono, T., Koketsu, S., Murata, A., Kawano, T. 2014. Southward spreading of the Fukushima-derived radiocesium across the Kuroshio Extension in the North Pacific. Scientific Reports 4: 4276. http://doi.org/10.1038/srep04276

Kumamoto, Y., Aoyama, M., Hamajima, Y., Nishino, S., Murata, A., Kikuchi, T. 2015. Meridional distribution of Fukushima-derived radiocesium in surface sea water along a trans-Pacific line from the Arctic to Antarctic Oceans in summer 2012. Journal of Radioanalytical and Nuclear Chemistry 307: 1703–1710. h ttps://doi.org/10.1007/s10967-015-4439-0

Kuroda, H., Wagawa, T. Shimizu, Y. Ito, S. Kakehi, S. Okunishi, T., Ohno, S., Kusaka, A. 2015. Interdecadal decrease of the Oyashio transport on the continental slope off the southeastern coast of Hokkaido, Japan. Journal of Geophysical Research Oceans 120: 2504–2522. https://doi.org/10.1002/2014JC010402

Kuroda, H., Wagawa, T., Kakehi, S., Shimizu, Y., Kusaka, A., Okunishi, T., Hasegawa, D., 2017. Long-term mean and seasonal variation of altimetry-derived Oyashio transport across the A-line off the southeastern coast of Hokkaido, Japan Deep-Sea Research Part I 121: 95–109. https://doi.org/10.1016/j.dsr.2016.12.006

Mantua, N.J., Hare, S.R., Zhang, Y., Wallace, J.M., Francis, R.C. 1997. A Pacific interdecadal climate oscillation with impacts on salmon production. Bulletin of the American Meteorological Society 78: 1069–1079. https://doi.org/10.1175/1520-0477(1997)078<1069:APICOW>2.0.CO;2

Men, W., He, J., Wang, F., Wen, Y., Li, Y., Huang, J., Yu, X. 2015. Radioactive status of seawater in the northwest Pacific more than one year after the Fukushima nuclear accident. Scientific Reports 5: 7757. https://doi.org/10.1038/srep07757

Minobe, S. 1997. A 50–70 year climatic oscillation over the North Pacific and North America. Geophysical Research Letters 24: 683–686. https://doi.org/10.1029/97GL00504

Minobe, S. 1999. Resonance in bidecadal and pentadecadal climate oscillations over the North Pacific: Role in climatic regime shifts. Geophysical Research Letters 26: 855–858. https://doi.org/10.1029/1999GL900119

Minobe, S. 2002. Interannual to interdecadal changes in the Bering Sea and concurrent 1998/99 changes over the North Pacific. Progress in Oceanography 55: 45–64. https://doi.org/10.1016/S0079-6611(02)00069-1

Miyama, T., Mitsudera, H., Nishigaki, H., Furue, R. 2018. Dynamics of a quasi-stationary jet along the subarctic front in the North Pacific Ocean (the western Isoguchi Jet): An ideal two-layer model. Journal of Physical Oceanography 48: 807–830. https://doi.org/10.1175/JPO-D-17-0086.1

Mitsudera H., Miyama, T., Nishigaki, H., Nakanowatari, T., Nishikawa, H., Nakamura, T., Wagawa, T., Furue, R., Fujii, Y., Ito, S. 2018. Low ocean-floor rises regulate subpolar sea surface temperature by forming baroclinic jets. Nature Communication 9: 1190. https://doi.org/10.1038/s41467-018-03526-z

Morita, K. 2014. Japanese wild salmon research: toward a reconciliation between hatchery and wild salmon management. North Pacific Anadromous Fish Commission Newsletter 35: 4–14.

Muto, M.M., Helker, V.T., Delean, B.J., Young, N.C., Freed, J.C., Angliss, R.P., Friday, N.A., Boveng, P.L., Breiwick, J.M., Brost, M.F., Cameron, M.F., Clapham, P.J., Crance, J.L., Dahle, S.P., Dahlheim, M.E., Fadely, B.S., Ferguson, M.C., Fritz, L.W., Goetz, K.T., Hobbs, R.C., Ivashchenko, Y.V., Kennedy, A.S., London, J.M., Mizroch, S.A., Ream, R.R., Richmond, E.L., Shelden, K.E.W., Sweeney, K.L., Towell, R.G., Wade, P.R., Waite, J.M., Zerbini, A.N. 2021. Alaska marine mammal stock assessments, 2020. U.S. Department of Commerce, NOAA Technical Memorandum, NMFS-AFSC-421, 398 p.

Nagasawa, K., Mayama, H. 1997. Additional fish predators of juvenile chum salmon (*Oncorhynchus keta*) in coastal waters of Japan, with a note on the importance as predators of juvenile masu salmon (*O. masou*). Technical Reports of Hokkaido Salmon Hatchery 166: 29–33 (In Japanese with English abstract).

Nakanowatari, T., Oshima, K.I., Wakatsuchi, M. 2007. Warming and oxygen decrease of intermediate water in the northwestern North Pacific, originating from the Sea of Okhotsk, 1955–2004. Geophysical Research Letters 34: L04602. https://doi.org/10.1029/2006GL028243

Nishikawa, H. Yasuda, I. 2008. Japanese sardine (*Sardinops melanostictus*) mortality in relation to the winter mixed layer depth in the Kuroshio Extension region. Fisheries Oceanography 17: 411–420. https://doi.org/10.1111/j.1365-2419.2008.00487.x

NPAFC Statistics. 2017. Pacific salmonid catch and hatchery release data (page updated August 11, 2017) (http://www.npafc.org/new/science_statistics.html).

Odate, T., Maita, Y. 1988. Regional variation in the size composition of phytoplankton communities in the Western North Pacific Ocean, spring 1985. Biological Oceanography 6: 65–77. https://doi.org/10.1080/01965581.1988.10749523

Ono T., Midorikawa, T., Watanabe, W.Y., Tadokoro, K. Saino, T. 2001. Temporal increases of phosphate and apparent oxygen utilization in the subsurface waters of western subarctic Pacific from 1968 to 1998. Geophysical Research Letters 28(17): 3285–3288. https://doi.org/10.1029/2001GL012948

Ono, T., Tadokoro, K., Midorikawa, T., Nishioka, J., Sano, T. 2002. Multi-decadal decrease of net community production in western subarctic North Pacific. Geophysical Research Letters 29: 8, 1186. https://doi.org/10.1029/2001GL014332

Ono, T., Kitagawa, D., Ito, M., Hattori, T., Narimatsu, Y. 2011. Oxygen decline in the continental slope waters off-Japan and its potential influence on groundfishes. Demersal Fish Studies in Tohoku Prefecture 31: 93–98 (in Japanese).

Osafune, S., Yasuda, I. 2006. Bidecadal variability in the intermediate waters of the northwestern subarctic Pacific and the Okhotsk Sea in relation to 18.6-year period nodal tidal cycle. Journal of Geophysical Research 111: C05007. https://doi.org/10.1029/2005JC003277

Pope, J.G., Shepherd, J.G., Webb, J. 1994. Successful surf-riding on size spectra: the secret of survival in the sea. Philosophical Transactions of the Royal Society of London, B 343: 41–49. https://doi.org/10.1098/rstb.1994.0006

Povinec, P.P., Hirose, K., Honda, T., Ito, T., Marian Scot, E., Togawa, O. 2004. Spatial distribution of ^{3}H, ^{90}Sr, ^{137}Cs and $^{239,240}Pu$ in surface waters of the Pacific and Indian Oceans-GLOMARD database. Journal of Environmental Radioactivity 76: 113–137. https://doi.org/10.1016/j.jenvrad.2004.03.022

Renaud, M.L. 1986. Hypoxia in Louisiana coastal waters during 1983. Fisheries Bulletin 84: 19–26.

Saito, H., Tsuda, A., Kasai, H. 2002. Nutrient and plankton dynamics in the Oyashio region of the western subarctic Pacific Ocean. Deep-Sea Research Part-II 49: 5463–5486. https://doi.org/10.1016/S0967-0645(02)00204-7

Saito, T., Hirabayashi, Y., Suzuki, K., Watanabe, K., Saito, H. 2016. Recent decline of pink salmon (*Onchorhynchus gorbuscha*) abundance in Japan. North Pacific Anadromous Fish Commission Bulletin 6: 279–296. https://doi.org/10.23849/npafcb6/279.296

Sasano, D., Takatani, Y., Kosugi, N., Nakano, T., Midorikawa, T., Ishii, M. 2018. Decline and bidecadal oscillations of dissolved oxygen in the Oyashio region and their propagation to the western North Pacific. Global Biogeochemical Cycles 32: 909–931. https://doi.org/10.1029/2017GB005876

Smith, J.N., Brown, R.M., Williams, W.J., Robert, M., Nelson, R., Moran, S.B. 2014. Arrival of the Fukushima radioactivity plume in North American continental waters. Proceedings of the National Academy of Sciences of the United States of America 112:1310–1315. https://doi.org/10.1073/pnas.1412814112

Sogawa, S., Sugisaki, H., Saito, H., Okazaki, Y., Shimode, S., Kikuchi, T. 2013. Congruence between euphausiid community and water region in the northwestern Pacific: particularly in the Oyashio–Kuroshio Mixed Water Region. Journal of Oceanography 69: 71–85. https://doi.org/10.1007/s10872-012-0158-0

Sogawa, S., Sugisaki, H., Saito, H., Okazaki, Y., Ono, T., Shimode, S., Kikuchi, T. 2016. Seasonal and regional change in vertical distribution and diel vertical migration of four euphausiid species (*Euphausia pacifica*, *Thysanoessa inspinata*, *T.longipes*, and *Tessarabrachion oculatum*) in the northwestern Pacific. Deep-Sea Research Part-I 109: 1–9. https://doi.org/10.1016/j.dsr.2015.12.010

Sugisaki, H. et al. 2010. Status and trends of the Kuroshio Current region, 2003-2008. pp. 330–359. In S.M. Mckinnell and M.J. Dagg [Eds] Marine Ecosystems of the North Pacific Ocean, 2003-2008. PICES Special Publication No. 4, 393 p.

Tadokoro, K., Chiba, S., Ono, T., Midorikawa, T., Saino, T. 2005. Interannual variation in *Neocalanus* biomass in the Oyashio waters of the western North Pacific. Fisheries Oceanography 14: 210–222. https://doi.org/10.1111/j.1365-2419.2005.00333.x

Tadokoro, K., Ono, T., Yasuda, I., Osafune, S., Shiomoto, A. and Sugisaki, H. 2009. Possible mechanisms of decadal-scale variation in PO_4 concentration in the western North Pacific. Geophysical Research Letters 36: L08606. https://doi.org/10.1029/2009GL037327

Takatani, Y., Sasano, D., Nakano, T., Midorikawa, T., Ishii, M. 2012. Decrease of dissolved oxygen after the mid-1980s in the western North Pacific subtropical gyre along the 137°E repeat section. Global Biogeochemical Cycles 26: GB2013. https://doi.org/10.1029/2011GB004227

Taki, K. 2012. Distribution and population structure of *Thysanoessa inspinata* and its dominance among euphausiids off northeastern Japan. Journal of Plankton Research 33: 891–906. https://doi.org/10.1093/plankt/fbq162

Trenberth, K.E., Hurrell, J.W. 1994. Decadal atmosphere-ocean variations in the Pacific. Climate Dynamics 9: 303–319. https://doi.org/10.1007/BF00204745

Vaquer-Sunyer, R., Duarte, C.M. 2008. Thresholds of hypoxia for marine biology. Proceedings of the National Academy of Sciences the United States of America 105: 15452–15457. https://doi.org/10.1073/pnas.0803833105

Wagawa, T., Ito, S., Shimizu, Y., Kakehi, S., Ambe, D. 2014. Currents associated with the quasi-stationary jet separated from the Kuroshio Extension. Journal of Physical Oceanography 44: 1636–1653. https://doi.org/10.1175/JPO-D-12-0192.1

Wagawa, T., Tamate, T., Kuroda, H., Ito, S., Kakei, S., Yamanome, T., Kodama, T. 2016. Relationship between coastal water properties and adult return of chum salmon (*Oncorhynchus keta*) along the Sanriku coast, Japan. Fisheries Oceanography 25: 598–609. https://doi.org/10.1111/fog.12175

Watanabe, Y., Zenitani, H. and Kimura, R. 1996. Offshore expansion of spawning of the Japanese sardine, *Sardinops melanostictus*, and its implication for egg and larval survival. Canadian Journal of Fisheries and Aquatic Sciences 53: 55–61. https://doi.org/10.1139/f95-153

Whitney, F. A. . 2011. Nutrient variability in the mixed layer of the subarctic Pacific Ocean, 1987-2010. Journal of Oceanography 67: 481–492. https://doi.org/10.1007/s10872-011-0051-2

Yasuda, I. 1997. The origin of the North Pacific Intermediate Water. Journal of Geophysical Research 102: C1, 893–909. https://doi.org/10.1029/96JC02938

Yasuda I, Okuda, K., Shimizu, Y. 1996. Distribution and modification of North Pacific intermediate water in the Kuroshio–Oyashio interfrontal zone. Journal of Physical Oceanography 26: 448–465. https://doi.org/10.1175/1520-0485(1996)026<0448:DAMONP>2.0.CO;2

Yasunaka, S., Hanawa, K. 2002. Regime shifts found in the Northern Hemisphere SST field. Journal of the Meteorological Society of Japan 80: 119–135. https://doi.org/10.2151/jmsj.80.119

Yasunaka, S., Hanawa, K. 2003. Regime shifts in the Northern Hemisphere SST field: Revisited in relation to tropical variations. Journal of the Meteorological Society of Japan 81: 415–424. https://doi.org/10.2151/jmsj.81.415

Yasunaka, S., Hanawa, K. 2005. Regime shift in the global sea-surface temperatures: Its relation to El Nino-southern oscillation events and dominant variation modes. International Journal of Climatology 25: 913–930. https://doi.org/10.1002/joc.1172

Yeh, S.-W., Kang, Y.-J., Noh, Y., Miller, A.J. 2011. The North Pacific climate transitions of the winters of 1976/77 and 1988/89. Journal of Climate 24: 1170–1183. https://doi.org/10.1175/2010JCLI3325.1

Yoshida, S., Macdonald, A.M., Jayne, S.R., Rypina, I.I., Buesseler, K.O. 2015. Observed eastward progression of the Fukushima ^{134}Cs signal across the North Pacific. Geophysical Research Letters 42: 7139–7147. https://doi.org/10.1002/2015GL065259

Zhang, Y., Wallace, J.M., Battisti, D.S. 1997. ENSO-like interdecadal variability: 1900–93. Journal of Climate 10: 1004–1020. https://doi.org/10.1175/1520-0442(1997)010<1004:ELIV>2.0.CO;2